

Suprasubduction-zone ophiolite generation, emplacement, and initiation of subduction: A perspective from geochemistry, metamorphism, geochronology, and regional geology

John Wakabayashi^{1,†}, Arundhuti Ghatak², and Asish R. Basu²

¹*Department of Earth and Environmental Sciences, California State University, Fresno, California 93740, USA*

²*Department of Earth and Environmental Sciences, University of Rochester, Rochester, New York 14627, USA*

ABSTRACT

Ophiolites are on-land remnants of oceanic lithosphere, and most of the more extensive ophiolites apparently formed above a subduction zone, a tectonic setting known as a suprasubduction-zone setting. Thin sheets of high-grade metamorphic rocks, known as metamorphic soles, crop out structurally beneath many suprasubduction-zone ophiolites. Such rocks may have formed during the inception of subduction beneath young and hot oceanic lithosphere. Disagreement exists as to whether suprasubduction-zone ophiolites are emplaced over the same subduction zone over which they once formed or over a later one. High-grade metamorphic rocks (blocks-in-mélange and coherent sheets) from the Franciscan Complex may represent a metamorphic sole beneath the suprasubduction-zone Coast Range ophiolite. Trace-element and isotopic data indicate that the Franciscan high-grade metamorphic rocks formed in a suprasubduction-zone environment, requiring the existence of a pre-Franciscan subduction zone, whereas later-subducted, lower-grade oceanic rocks are of mid-ocean-ridge or oceanic-island basalt affinities. The Coast Range ophiolite and Franciscan high-grade rock protoliths formed over a pre-Franciscan subduction zone that may have dipped westward. The high-grade Franciscan rocks were metamorphosed at the inception of east-dipping subduction beneath the Coast Range ophiolite, and the ophiolite was subsequently emplaced over this later subduction zone. Suprasubduction-zone protolith signatures have been obtained for other metamorphic soles beneath suprasubduction-zone ophiolites, suggesting that our proposed model of

suprasubduction-zone ophiolite generation over one subduction zone and emplacement over a second one may be globally applicable. Regional geology suggests that this dual subduction-zone model may also apply to suprasubduction-zone ophiolites with mid-ocean-ridge and/or oceanic-island basalt soles.

INTRODUCTION

Many of the world's best-known ophiolites (on-land remnants of oceanic lithosphere) have petrologic and geochemical characteristics that suggest formation above a subduction zone, an environment of formation known as a suprasubduction-zone environment (e.g., Pearce et al., 1984). In addition, many suprasubduction-zone ophiolites appear to have been formed shortly after the initiation of subduction in a nascent arc environment, where oceanic crust formed in concert with significant extension over a subducting slab that was rolling back (Stern and Bloomer, 1992). Most ophiolite researchers ascribe to the tectonic model of Stern and Bloomer (1992) or variations on that model (e.g., Shervais, 2001; Dilek and Flower, 2003), in which emplacement of the suprasubduction-zone ophiolite takes place over the same subduction zone above which the ophiolite formed (Fig. 1). In this paper, we refer to emplacement of suprasubduction-zone ophiolites as occurring (1) when the ophiolite is thrust over a continental margin, as a result of failed subduction of the continental margin beneath it (the case for typical Tethyan ophiolites), or (2) over a subduction complex (the case for many circum-Pacific ophiolites) (Wakabayashi and Dilek, 2003). This definition does not include the emplacement mechanisms of some Appalachian suprasubduction-zone ophiolites that were emplaced into an orogenic belt as large sheets by partial subduction (Zagorevski et al., 2006; Lissenberg et al., 2005), or incorporation

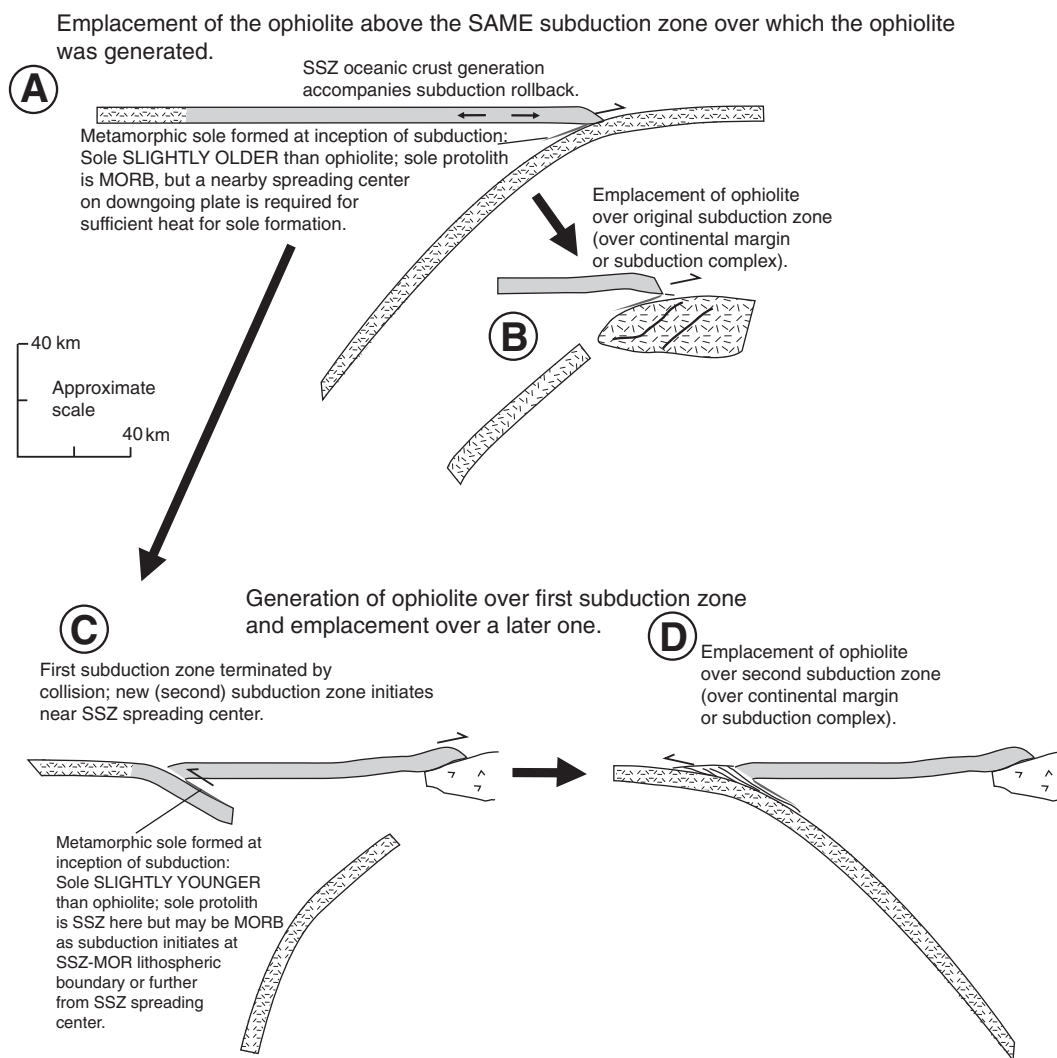
of smaller fragments of oceanic lithosphere into accretionary prisms (Franciscan-style ophiolites of Dilek, 2003).

In contrast to the widely accepted model in which ophiolite genesis and emplacement occur over the same subduction zone, Wakabayashi and Dilek (2000, 2003) proposed that suprasubduction-zone ophiolites form over one subduction zone but are emplaced over a different one (Fig. 1). Accordingly, the rock record of subduction initiation should offer important insight into their generation and emplacement.

Thin (usually a few hundred meters thick or less) sheets of high-grade metamorphic rocks, known as metamorphic soles, have been found structurally beneath many of the world's suprasubduction-zone ophiolites, and these high-grade rocks are suggested to have formed at the inception of subduction in young (near a spreading center) oceanic crust (Williams and Smyth, 1973; Spray, 1984; Jamieson, 1986; Hacker, 1991; Hacker et al., 1996). The environment of suprasubduction-zone ophiolite generation influences the temporal relationship between ophiolite and sole formation (Wakabayashi and Dilek, 2000). If the suprasubduction-zone ophiolite formed after the subduction initiation event recorded by the metamorphic sole, then the ophiolite formed over the same subduction zone over which it was emplaced, consistent with the model of Stern and Bloomer (1992) (Fig. 1). If the ophiolite formed prior to the formation of the metamorphic sole, then it could not have formed over the subduction zone that did not exist until the formation of that sole. The difference in suprasubduction-zone ophiolite generation and emplacement models appears resolvable with geochronology alone, but difficulties arise in the application of geochronologic techniques because (Wakabayashi and Dilek, 2000): (1) The most reliable and available metamorphic ages obtained from metamorphic soles are Ar/Ar hornblende ages that are cooling dates, because

[†]E-mail: jwakabayashi@csufresno.edu

Figure 1. Diagrams showing the difference between a model where a suprasubduction-zone (SSZ) ophiolite is emplaced over the same subduction zone above which it was generated (sequence A-B; a single subduction-zone model), and a scenario in which the suprasubduction-zone ophiolite is generated above one subduction zone and emplaced over a different one (sequence A-C-D; dual subduction-zone model). Note that with a nascent arc setting for the suprasubduction-zone ophiolite shown, the second subduction zone is most likely to be of opposite polarity in order for the suprasubduction-zone spreading center (with younger, less dense lithosphere) to be on the hanging wall. For suprasubduction-zone spreading centers in intra-arc or back-arc settings, there are more permissible geometries for a second subduction zone of the same polarity as the first because of the greater across-strike distance between the first subduction zone and the suprasubduction-zone spreading center. MORB—mid-ocean-ridge basalt.



the temperature of sole metamorphism exceeded the closure temperature for Ar in hornblende. (2) The most reliable igneous (formation) ages from ophiolites are U/Pb zircon ages, most of which are obtained from plagiogranites that may have formed fairly late in the evolution of the ophiolite. (3) The igneous age of the ophiolite and the metamorphic age of the sole obtained with the previous two methods are commonly within analytical error of each other. Although Hacker et al. (1996) and Wakabayashi and Dilek (2000) have argued that the geochronologic, metamorphic, and field data suggest that the suprasubduction-zone ophiolite formed slightly before the sole did, the data may permit the alternative interpretation, that the sole formed first.

Geochemistry enables us to further explore the relationship between subduction initiation, suprasubduction-zone ophiolite formation, and suprasubduction-zone ophiolite emplacement. Saha et al. (2005) showed that high-grade metamorphic blocks-in-mélange from Tiburon Penin-

sula of the Franciscan Complex, California, have suprasubduction-zone protoliths. These high-grade metamorphic blocks have been interpreted as the dismembered remnants of a metamorphic sole (Platt, 1975; Cloos, 1985; Wakabayashi, 1990). The protoliths of the blocks apparently formed over a subduction zone that predated the one that began with the high-grade metamorphism recorded in them (Franciscan subduction). However, an alternative model links Franciscan high-grade metamorphism, and metamorphic sole formation in general, to ridge subduction rather than subduction initiation (Shervais, 2001; Shervais et al., 2005). In addition, a study by Saha et al. (2005) examined metamorphic blocks from only one of hundreds of Franciscan localities, so it is not clear how representative the single locality is of general Franciscan high-grade metamorphism.

In this study, we present new data from multiple high-grade Franciscan metamorphic localities, including coherent thrust sheets and

blocks-in-mélange, and we show that Franciscan high-grade protoliths appear to have been mostly suprasubduction-zone basalts, with some mid-ocean-ridge basalt (MORB). We will argue that the geochemical data indeed capture protolith environments and do not represent an artifact generated by element mobility during metamorphism. We also review the metamorphic and field evidence and conclude that the field relations and metamorphic conditions indicate that high-grade Franciscan metamorphism formed as a product of subduction initiation, rather than ridge subduction. An important additional piece of evidence is the recent identification of high-grade coherent thrust sheets (Wakabayashi and Dumitru, 2007) from which some of the new geochemical data are derived, because the tectonic history of coherent thrust sheets is more constrained than that of blocks-in-mélange. Our study corroborates the suggestion by Saha et al. (2005) that the Franciscan high-grade metamorphic rocks and the Coast

Range ophiolite formed over a subduction zone that predated Franciscan subduction. We then explore the applicability of this model to other suprasubduction-zone ophiolites.

FRANCISCAN COMPLEX METAMORPHISM AND GEOLOGIC SETTING

The Franciscan Complex of California formed during a period of over 140 m.y. of continuous east-dipping subduction in coastal

California from 160 Ma to younger than 20 Ma (Ernst, 1984; Wakabayashi, 1992). The Franciscan Complex is well known for its high-pressure–low-temperature (high P –low T) metamorphism (Ernst, 1970, 1971b) and mélangé (Hsü, 1968). At least 25% of the exposed rocks have undergone high P –low T , blueschist-grade, or higher, metamorphism (Wakabayashi, 1999).

The Coast Range ophiolite, consisting of serpentinized ultramafic rocks, gabbro, basalt, and other plutonic and volcanic rocks, structur-

ally overlies the Franciscan Complex (Hopson et al., 1981) and is depositionally overlain by well-bedded sandstones and shales of the Great Valley Group, which are coeval with the clastic sedimentary rocks of the Franciscan Complex (Dickinson, 1970). The Coast Range ophiolite and Great Valley Group lack high P –low T metamorphism. From west to east, the three subparallel geologic provinces of the Franciscan, Great Valley Group, and the Sierra Nevada batholith (Fig. 2) represent, respectively, the subduction complex, forearc basin deposits, and the

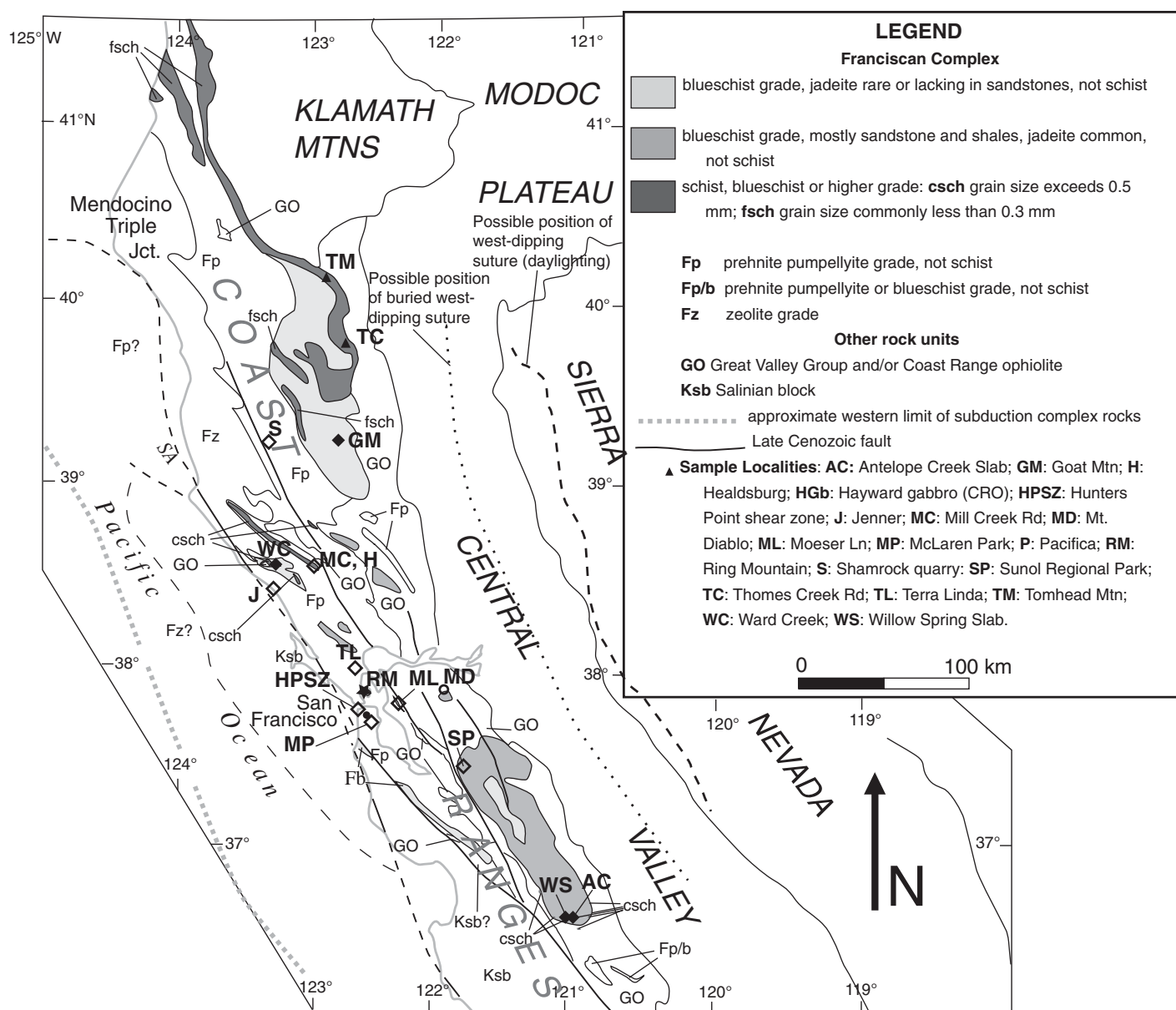


Figure 2. Distribution of Franciscan and related rocks of central and northern California, showing sample localities discussed in this proposal (modified from Wakabayashi, 1999). Sample field relations and tectonic affinity are denoted by: high-grade coherent sheets (filled diamonds), high-grade tectonic blocks (open diamonds), low-grade coherent sheets (filled triangles), and Coast Range ophiolite (open circles). The Ring Mountain high-grade block locality, where (multiple) blocks were analyzed by Saha et al. (2005), is marked with a star.

magmatic arc of an ancient arc-trench system (Dickinson, 1970). Franciscan lithologies are predominantly detrital sedimentary rocks, with subordinate basaltic volcanic rocks and chert, and minor limestone (Bailey et al., 1964; Blake et al., 1988). The detrital rocks are off-scraped and underplated trench-fill sediments (Dickinson, 1970). The pelagic and volcanic rocks apparently represent fragments of seamounts, other oceanic rises, and the pelagic cover and upper part of the subducted oceanic crust (Hamilton, 1969; MacPherson, 1983; Shervais, 1990), probably with a component of olistostrome blocks from the upper plate (MacPherson et al., 1990; Erickson et al., 2004).

Franciscan rocks have been traditionally classified as internally “coherent” mappable bodies or *mélange* units that consist of a sheared matrix with included blocks (Blake et al., 1988; Wakabayashi, 1992, 1999). *Mélange* blocks may reach sizes of kilometers in map dimensions, so coherent units are not defined on the basis of a minimum size, but rather by their scaling compared to the shear zones or contacts that bound them. A coherent unit is one that is vastly greater in dimension than the thickness (width) of any shear zones that bound it. Metamorphism in coherent terranes ranges from zeolite facies to epidote blueschist (Blake et al., 1988), with the exception of rare high-grade slabs that display eclogite, amphibolite, and garnet-amphibolite assemblages; tectonic blocks-in-*mélange* span the same range in metamorphism (Wakabayashi and Dumitru, 2007). It is useful to define “high-grade” metamorphic rocks to include blocks-in-*mélange* (referred to as “high-grade blocks”) and their rare coherent equivalents. Collectively, the high-grade metamorphic rocks make up far less than 1% of Franciscan metamorphic rocks, but they are very widely distributed, cropping out at hundreds of localities along the length of the subduction complex (Coleman and Lanphere, 1971). Many, if not most, of eclogites have relics of earlier amphibolite-facies metamorphic assemblages (Moore and Blake, 1989; Wakabayashi, 1990). High-grade rocks are entirely metabasites with minor metacherts, whereas lower-grade coherent metamorphic rocks are mostly meta-graywackes and metashales, with lesser proportions of metabasites and metacherts (Blake et al., 1988; Coleman and Lanphere, 1971). Many high-grade blocks are partly encased in “rinds” composed of minerals such as actinolite, chlorite, talc, and phengite: this rind apparently formed by metasomatic reaction between the block and the ultramafic rocks under conditions of decreasing metamorphic grade (e.g., Coleman and Lanphere, 1971; Moore, 1984). High-grade metamorphism evolved

along a counterclockwise *P-T* path (*P* on the positive *y*-axis; Wakabayashi, 1990; Krogh et al., 1994; Tsujimori et al., 2006; Page et al., 2007), whereas metamorphism in lower-grade metamorphic rocks took place under a mildly clockwise or hairpin *P-T* trajectory (Maruyama and Liou, 1988; Maruyama et al., 1985).

The high-grade rocks are the oldest metamorphic rocks in the Franciscan, yielding Ar/Ar hornblende ages of 157–163 Ma (Ross and Sharp, 1988; Wakabayashi and Dumitru, 2007), Lu-Hf garnet ages of 153–169 Ma (Anczkiewicz et al., 2004), and lower-temperature metamorphic or cooling ages ($^{40}\text{Ar}/^{39}\text{Ar}$ or K/Ar white mica) of 138–159 Ma (Wakabayashi and Deino, 1989; Wakabayashi and Dumitru, 2007). The age of high-temperature metamorphism in the high-grade rocks is slightly younger than the crystallization age of the 165–172 Ma Coast Range ophiolite and associated rocks (Shervais et al., 2005; Hopson et al., 2008).

Ages of lower-grade blueschist metamorphism (either metamorphic or cooling) range from ca. 135 Ma to 80 Ma (Wakabayashi and Dumitru, 2007). Peak temperatures of Franciscan metamorphism decrease with decreasing age, from amphibolites with temperatures of over 600 °C in the high-grade blocks (Wakabayashi, 1990) to 300–350 °C for epidote blueschists (Blake et al., 1988; Maruyama and Liou, 1988) at 154 Ma (Wakabayashi and Dumitru, 2007) to 150–250 °C for lawsonite blueschist-facies rocks (Ernst, 1971a; Maruyama et al., 1985) at 80–120 Ma (Wakabayashi and Dumitru, 2007), and ultimately to zeolite and prehnite-pumpellyite temperatures of <200 °C (Blake et al., 1988) for the last 95 Ma. Peak metamorphic pressures of high-grade metamorphic rocks range from ~5 kbar for the lowest pressure amphibolites (Wakabayashi, 1990) to 20–25 kbar for eclogites (Tsujimori et al., 2006; Page et al., 2007). Lower-grade blueschist gives pressures of ~6 to >10 kbar (Maruyama et al., 1985; Ernst, 1993), whereas sub-blueschist-grade rocks were metamorphosed at pressures at 4 kbar or less (Blake et al., 1988). Metamorphic ages (true metamorphic ages rather than cooling ages) of Franciscan rocks approximate the time of subduction because exhumation of these rocks occurred while subduction and refrigeration were ongoing (Ernst, 1988).

The high-grade rocks have been suggested to be the remnants of a metamorphic sole formed at the inception of subduction beneath hot sub-oceanic upper-mantle material, based on their old age, their age relative to the Coast Range ophiolite, lithology, presence of actinolite-chlorite rinds around high-grade blocks, and counterclockwise pressure-temperature (*P-T*)

evolution, whereas lower-grade Franciscan rocks formed during subsequent subduction (Wakabayashi, 1990). The high-grade rocks thus are analogous to sheets of high-grade rocks found beneath ophiolites called metamorphic soles (Platt, 1975; Wakabayashi, 1990; Wakabayashi and Dilek, 2000).

Lower-grade coherent volcanic rocks of the Franciscan Complex exhibit predominantly ocean-island basalts (OIB), with some rocks of mid-ocean-ridge (MORB) chemistry (MacPherson et al., 1990; Shervais, 1990; Shervais and Kimbrough, 1987), whereas lower-grade tectonic blocks-in-*mélange* (fine-grained blueschist and lower in grade) include OIB, MORB, and island-arc chemistry (MacPherson et al., 1990). Geochemical characteristics of coherent epidote blueschists from Ward Creek (Fig. 2), a unit that has yielded a white mica $^{40}\text{Ar}/^{39}\text{Ar}$ age of 154 Ma (Wakabayashi and Dumitru, 2007), have been interpreted as suggesting island-arc (i.e., suprasubduction-zone) protoliths (Swanson et al., 2004). Because the white mica age of the Ward Creek is within the range of the high-grade rocks, we group these rocks with them for purposes of discussion, even though the metamorphic grade of Ward Creek rocks is the same as the other blueschist-facies coherent rocks we analyzed from the South Fork Mountain schist. Saha et al. (2005) showed that high-grade blocks from Tiburon Peninsula exhibited geochemistry that indicated suprasubduction-zone protoliths. In contrast to most of the volcanic rocks in the Franciscan, the Coast Range ophiolite exhibits island-arc chemistry and is thought to represent the early stages of arc development (Shervais and Kimbrough, 1985; Stern and Bloomer, 1992; Shervais, 1990; Giaramita et al., 1998; Shervais, 2001).

NEW GEOCHEMICAL DATA FROM FRANCISCAN METAMORPHIC ROCKS

Major- and trace-element concentrations and high-precision Sr-, Nd-, and Pb-isotopic ratios of 25 Franciscan samples and one Coast Range ophiolite sample were analyzed for this study. These samples include samples from high-grade blocks (Moeser Lane, Mill Creek Road, Jenner, Shamrock Quarry, Terra Linda, Hunter's Point, Sunol, Healdsburg), high-grade coherent sheets (Panoche Pass [two different slabs: the Willow Spring slab and the Antelope Creek slab], Goat Mountain, Ward Creek), low-grade coherent sheets (Thomes Creek Road, Tomhead Mountain), and Coast Range ophiolite (CRO) basalt from Mt. Diablo (Fig. 2). The sample numbers and their corresponding rock names and tectonic affinities are reported in Table 1.

TABLE 1. ROCK NAMES, LOCALITIES, AND TECTONIC AFFINITIES OF FRANCISCAN SAMPLES OF THIS STUDY

Sample no.	Rock type	Locality	Tectonic affinity
F-1	Garnet amphibolite	Moeser Lane	High-grade tectonic block
F-3	Garnet amphibolite	Antelope Creek Slab	High-grade coherent sheet
F-4	Garnet blueschist	Jenner	High-grade tectonic block
F-6	Garnet amphibolite	Shamrock Quarry	High-grade tectonic block
F-8	Eclogite	Jenner	High-grade tectonic block
F-9	Epidote blueschist	Thomes Creek Road	Low-grade coherent sheet
F-10	Epidote blueschist	Mill Creek Road	High-grade tectonic block
F-11	Eclogite	Mill Creek Road	High-grade tectonic block
F-12	Epidote blueschist	Thomes Creek Road	Low-grade coherent sheet
GM-2	Garnet amphibolite	Goat Mountain	High-grade coherent sheet
GM-3	Garnet amphibolite	Goat Mountain	High-grade coherent sheet
WC-MV-1	Epidote blueschist	Ward Creek	High-grade coherent sheet
WC-MV-2	Epidote blueschist	Ward Creek	High-grade coherent sheet
95-DIAB-107c	Eclogite	Willow Spring Slab	High-grade coherent sheet
95-DIAB-14	Lawsonite blueschist	Willow Spring Slab	High-grade coherent sheet
95-DIAB-031	Eclogite	Willow Spring Slab	High-grade coherent sheet
95-DIAB-29	Epidote blueschist	Willow Spring Slab	High-grade coherent sheet
Mt. Diab-1	Basalt	Mt. Diablo	Coast Range ophiolite
TL-4	Amphibolite	Terra Linda	High-grade tectonic block
SFM-1	Epidote blueschist	Tomhead Mountain	Low-grade coherent sheet
SFM-6	Epidote blueschist	Tomhead Mountain	Low-grade coherent sheet
HPSZ	Garnet amphibolite	Hunter's Point	High-grade tectonic block
SUNOL-2038	Eclogite	Sunol	High-grade tectonic block
JS-Ecg	Gabbro	Healdsburg	High-grade tectonic block
MP-1	Eclogite	McLaren Park	High-grade tectonic block/ high-grade coherent sheet

Note: Sample localities are also shown in Figure 1.

ANALYTICAL METHODS

Whole-rock samples were powdered using a Spex alumina ball mill in our laboratory at the University of Rochester. Starting with a 1 kg rock sample, we broke them into chips and finally selected 10 g of these chips to be powdered for each sample to ensure that the powder was representative of the whole-rock sample.

A commercial laboratory was used for the analysis of major elements (Activation Laboratories Ltd., Ontario). All the other trace-element and isotopic analyses reported here were carried out at the University of Rochester.

Major-element concentrations of the samples were determined by ICP-OES (inductively coupled plasma–optical emission spectrometry) and are reported in Table 2. The samples underwent lithium metaborate/tetraborate fusion prior to measurements. Repeated measurements of known rock standards indicate that the concen-

trations of the major elements are within 0.1% of the known rock standard values, as certified by Activation Laboratories Ltd.

Trace-element concentrations were measured using an inductively coupled plasma–mass spectrometer (Thermo elemental X-7 series) at the University of Rochester. Samples of 25 mg powdered rock each were digested using HF–HNO₃ acid mixtures and diluted to a 100 mL solution with 2% HNO₃. Each sample was then spiked with a 10 ppb internal standard of In, Cs, Re, and Bi. BCR-2 (U.S. Geological Survey [USGS] basalt) was used as a known external standard, while AGV-2 (andesite-USGS) and BHVO-2 (basalt-USGS) rock standards were run as unknowns to estimate the error in the trace-element analyses reported here (Table 3). Analytical uncertainties were usually less than 5% for most of the trace elements and were commonly less than 2% for rare earth elements (REEs).

Nd-, Sr-, and Pb-isotopic ratios were measured with a multicollector thermal ionization mass spectrometer (TIMS; VG Sector at the University of Rochester) for which 100–200 mg powdered rock samples were dissolved in HF–HNO₃ and HCl acids. Nd- and Sr-isotopes were measured using the procedures established for our laboratory at the University of Rochester (Basu et al., 1990). Measured ⁸⁷Sr/⁸⁶Sr ratios were normalized to ⁸⁶Sr/⁸⁸Sr = 0.1194. Uncertainties for the measured ⁸⁷Sr/⁸⁶Sr ratios were less than ±0.00004. The NBS-987 Sr standard analyzed during the course of this study yielded ⁸⁷Sr/⁸⁶Sr = 0.710245 ± 0.000023 (2σ) (n = 5). Measured ¹⁴³Nd/¹⁴⁴Nd ratios were normalized to ¹⁴⁶Nd/¹⁴⁴Nd = 0.7219. Uncertainties for the measured ¹⁴³Nd/¹⁴⁴Nd ratios were less than ±0.00003. La Jolla Nd standard analyzed during the course of this study yielded ¹⁴³Nd/¹⁴⁴Nd = 0.511856 ± 0.000024 (2σ) (n = 4). Initial ε_{Nd} values were calculated using present-day bulk earth ¹⁴³Nd/¹⁴⁴Nd of 0.512638 and ¹⁴⁷Sm/¹⁴⁴Nd of 0.1968 (Jacobsen and Wasserburg, 1984). Pb isotopes were also measured in our laboratory in Rochester using the silica-gel technique (Sharma et al., 1992). Filament temperature during Pb-isotope ratio measurements was monitored continuously, and raw ratios were calculated as weighted averages of the ratios measured at 1150 °C, 1200 °C, and 1250 °C, respectively. The reported Pb-isotopic data were corrected for mass fractionation of 0.12 ± 0.03% per a.m.u. based on replicate analyses of the NBS-981 Equal Atom Pb standard measured in the same fashion. Estimated errors were less than 0.05% per mass unit. Our laboratory procedural blanks were <400 pg for Sr and <200 pg for both Nd and Pb. No blank correction was necessary for the isotope ratios reported in Table 4.

ANALYTICAL RESULTS

Major-element data for 9 of the 25 samples are given in Table 2. We present the major-element data mainly as a starting point, to help the reader visualize the general chemistry of these rocks,

TABLE 2. MAJOR-ELEMENT COMPOSITIONS OF SELECTED HIGH-GRADE BLOCKS, HIGH-GRADE COHERENT SHEETS, AND LOW-GRADE COHERENT SHEETS FROM DIFFERENT LOCALITIES OF THE FRANCISCAN COMPLEX

Sample	F-1	F-3	F-4	F-6	F-8	F-9	F-10	F-11	F-12
SiO ₂	53.71	44.54	47.58	50.33	46.34	45.64	48.37	44.63	47.22
Al ₂ O ₃	15.75	13.70	12.62	13.22	12.12	13.19	11.88	13.42	12.34
Fe ₂ O ₃ (T)	9.81	16.65	16.88	13.44	12.54	13.89	11.87	13.11	14.21
MnO	0.21	0.38	0.25	0.24	0.21	0.23	0.16	0.25	0.21
MgO	5.48	7.52	6.25	7.44	5.54	6.53	14.87	7.48	5.96
CaO	6.32	9.61	7.84	9.11	14.09	10.63	1.45	11.27	9.90
Na ₂ O	5.93	2.57	3.78	3.20	3.85	2.33	4.38	3.98	2.85
K ₂ O	0.27	0.19	0.13	0.21	0.40	0.04	0.73	0.48	< 0.01
TiO ₂	0.88	2.00	3.16	1.85	2.78	2.31	0.72	1.88	2.63
P ₂ O ₅	0.09	0.26	0.51	0.24	0.57	0.21	0.12	0.14	0.24
LOI	1.32	2.34	0.94	0.57	0.40	4.48	4.54	2.55	3.61
Total	99.77	99.75	99.95	99.84	98.84	99.49	99.10	99.18	99.16

Note: Major-element concentrations are in wt% with 0.01% analytical uncertainties. LOI—loss on ignition.

TABLE 3. TRACE-ELEMENT COMPOSITIONS OF SELECTED HIGH-GRADE BLOCKS, HIGH-GRADE COHERENT SHEETS, AND LOW-GRADE COHERENT SHEETS FROM DIFFERENT LOCALITIES OF THE FRANCISCAN COMPLEX

Sample	F-1	F-3	F-4	F-6	F-8	F-9	F-10	F-11	F-12	GM-2	GM-3	WC-MV-1	WC-MV-2
Rb	2.4	4.2	2.7	2.5	11.3	0.44	15	12	0.24	1.2	4.6	19	3.4
Ba	186	220	40	28	225	222	495	686	38	242	155	60	51
Sr	155	68	99	93	308	44	8.3	612	89	100	32	127	190
Pb	2.3	1.3	2.8	1.1	4.2	0.96	1.0	9.2	0.92	0.78	0.06	0.44	0.60
La	4.7	7.1	9.2	4.0	8.0	5.7	5.0	5.7	7.1	3.9	5.5	2.8	2.8
Ce	10.7	17	27	12	24	17	11	15	21	11	18	10	10
Pr	1.6	2.7	4.4	2.2	4.2	3.0	1.7	2.8	3.6	1.7	3.3	1.5	1.5
Nd	7.6	13	23	12.1	23	15	7.8	14	19	8.6	15	8.1	8.0
Sm	2.3	4.5	8.1	4.6	8.4	5.5	2.6	5.0	6.5	3.1	7.0	2.9	2.8
Eu	0.72	1.5	2.6	1.6	2.9	1.9	0.83	1.7	2.2	1.22	2.2	1.2	1.1
Gd	3.0	6.2	10.6	6.3	11.8	7.4	3.3	6.7	8.6	4.5	10.1	4.1	3.9
Tb	0.52	1.1	1.9	1.13	2.0	1.3	0.58	1.2	1.5	0.81	1.84	0.75	0.71
Dy	3.32	7.6	11	7.4	11.7	8.2	3.6	7.5	9.8	5.3	12	4.9	4.6
Ho	0.72	1.8	2.4	1.7	2.4	1.82	0.80	1.6	2.1	1.2	2.7	1.1	1.0
Er	1.98	5.4	6.3	4.8	6.7	5.1	2.3	4.7	5.9	3.3	7.5	2.9	2.8
Tm	0.30	0.87	0.94	0.73	0.98	0.75	0.35	0.67	0.84	0.51	1.1	0.43	0.42
Yb	1.98	5.9	6.0	4.7	6.3	4.8	2.3	4.4	5.2	3.3	7.7	2.7	2.7
Lu	0.29	0.91	0.86	0.70	0.95	0.66	0.34	0.63	0.7	0.48	1.2	0.38	0.39
Y	21	52	68	49	69	50	23	46	58	31	76	28	26
Th	0.61	0.64	0.41	0.20	0.43	0.23	0.69	0.29	0.26	0.37	0.54	0.13	0.12
U	0.15	0.16	0.29	0.29	1.2	0.09	0.18	0.11	0.16	0.24	0.43	0.17	0.08
Zr	6.1	19.5	5.4	3.2	6.4	70	4.8	9.1	55	16	24	4.5	2.8
Hf	0.38	0.95	0.34	0.20	0.32	2.2	0.19	0.60	1.8	0.79	1.2	0.23	0.16
Nb	3.0	10.7	6.0	0.89	5.2	4.2	2.5	4.3	3.2	3.2	12	2.1	2.2
Ta	0.16	0.65	0.37	0.07	0.30	0.27	0.15	0.25	0.17	0.20	0.70	0.13	0.14
Sc	33	50	40	42	44	46	29	45	44	55	58	42	42
V	239	456	508	412	562	419	282	396	429	382	523	275	279

Sample	95-DIAB-107c	95-DIAB-14	95-DIAB-031	95-DIAB-29	MT. Diab-1	TL-4	SFM-1	SFM-6	HPSZ	SUNOL-2038	JS-Ecg	MP-1
Rb	47	3.6	1.4	14	1.0	0.59	5.1	1.3	7.3	7.4	0.13	11
Ba	240	30	164	45	11	20	44	16	113	398	5.0	140
Sr	231	200	787	227	55	17	504	244	60	307	76	67
Pb	9.9	1.8	43	0.69	106	0.66	2.0	1.1	0.79	4.1	2.0	0.66
La	3.3	8.7	8.4	3.1	4.6	3.5	6.6	5.4	2.6	1.4	11	2.9
Ce	8.6	19	21	8.6	13	8.2	24	17.5	6.6	3.2	32	6.5
Pr	1.7	2.8	3.4	1.4	2.4	1.2	4.1	3.0	1.2	0.52	4.4	1.39
Nd	9.2	12	13	5.6	12	5.9	21	16	6.4	2.7	21	6.3
Sm	4.1	3.3	5.2	2.2	4.4	1.6	7.5	5.4	2.4	1.1	5.4	3.0
Eu	1.6	1.1	1.9	0.86	1.7	0.58	2.6	1.8	0.83	0.44	1.5	1.2
Gd	5.4	3.5	6.7	3.1	6.1	1.9	10	7.2	3.5	1.1	5.5	4.7
Tb	1.0	0.55	1.2	0.52	1.1	0.31	1.8	1.3	0.64	0.19	0.72	0.84
Dy	6.3	3.3	7.4	3.5	7.3	2.0	11	8.4	4.4	1.2	3.8	5.5
Ho	1.3	0.7	1.6	0.74	1.61	0.41	2.4	1.8	0.99	0.27	0.75	1.24
Er	3.5	2.0	4.5	2.0	4.6	1.2	6.3	5.0	3.0	0.79	2.0	3.5
Tm	0.50	0.29	0.65	0.30	0.70	0.17	0.88	0.74	0.46	0.12	0.29	0.52
Yb	3.1	1.8	4.2	1.9	4.6	1.1	5.5	4.5	3.1	0.86	1.9	3.4
Lu	0.44	0.25	0.6	0.27	0.68	0.16	0.66	0.59	0.45	0.13	0.29	0.52
Y	37	17	44	21	43	11	64	48	27	7.4	18	35
Th	0.37	1.4	0.73	0.21	0.36	-0.03	0.46	0.63	0.21	-0.23	1.0	0.16
U	0.39	0.42	0.38	0.16	0.18	-0.52	0.20	0.47	0.22	-0.47	0.09	0.19
Zr	3.0	7.3	6.9	2.7	123	10	47	57	16	4.7	6.6	16
Hf	0.21	0.25	0.30	0.11	3.4	0.47	2.1	1.9	0.83	0.24	0.40	0.86
Nb	1.9	1.8	10	3.7	4.6	0.78	6.3	5.6	2.6	0.73	1.3	1.9
Ta	0.08	0.14	0.58	0.26	0.25	0.03	0.36	0.24	0.12	0.02	0.06	0.11
Sc	50	26	53	31	48	35	66	41	45	48	57	46
V	368	1228	465	171	393	1322	433	483	296	468	463	348

Note: Trace-element concentrations are in ppm, and analytical uncertainties are within 5%.

and for comparative purposes, given that our evaluation of protolith affinities for these rocks is based on trace-element and isotopic data, as discussed later. The total alkali versus silica variations for these rocks are plotted in Figure 3, along with the previous published data of the high-grade rocks from our previous study (Saha et al., 2005) and the compositional ranges of some modern intra-oceanic arcs of the western Pacific. The SiO_2 contents of these rocks vary from 44.5% to 53.71% and the $(\text{Na}_2\text{O} + \text{K}_2\text{O})$ contents vary from 2.4% to 6.2%, indicating that these rocks fall along a calc-alkaline trend simi-

lar to those of orogenic belt basalts and basaltic andesites. The two low-grade coherent schists (epidote blueschists) from Thomes Creek Road (F-9 and F-12, Table 1) fall in the field of basalts, with the lowest Na and K. Based on major-element chemistry, these and other rocks falling in the field of basalts in Figure 3 may have either a normal (N)-MORB-like or an arc tholeiitic parentage; trace-element and isotopic data will be evaluated later herein to better distinguish the protolith affinity of the samples.

Major-element composition of rocks can only be considered diagnostic when coupled

with other isotopic and trace-element data due to the possibility that their major-element compositions could have been modified by seafloor and subduction-zone alteration processes. Some trace elements, such as the relatively immobile high field strength elements (HFSE) and the isotopes of Nd, Sr, and Pb, in combination, can delineate these processes. These characteristics were the essence of our geochemical approach in our previous study (Saha et al., 2005), and they are the foundation of this study.

Trace-element data for all the Franciscan rocks of this study are presented in Table 3.

TABLE 4. Rb, Sr, Sm, Nd, U, Th, AND Pb CONCENTRATIONS AND INITIAL Sr-Nd-Pb-ISOTOPE DATA AT 169 MA FOR SELECTED ROCKS OF THE FRANCISCAN COMPLEX

Sample	F-1	F-3	F-4	F-6	F-8	F-9	F-10	F-11	F-12	GM-2	GM-3	WC-MV-1	WC-MV-2
Sm (ppm)	2.3	4.5	8.1	4.6	8.4	5.5	2.6	5.0	6.5	3.1	7.0	2.9	2.8
Nd (ppm)	7.6	13.4	23	12	22.9	16	7.8	14	19	8.6	18	8.1	8.0
¹⁴⁷ Sm/ ¹⁴⁴ Nd	0.195	0.213	0.224	0.238	0.232	0.220	0.207	0.218	0.214	0.23	0.239	0.227	0.223
¹⁴³ Nd/ ¹⁴⁴ Nd(0)	0.51279	0.51295	0.51312	0.51319	0.51313	0.51325	0.51289	0.51289	0.51328	0.51290	0.51308	0.51304	0.51295
¹⁴³ Nd/ ¹⁴⁴ Nd(I)	0.51279	0.51295	0.51312	0.51319	0.51313	0.51325	0.51289	0.51289	0.51328	0.51265	0.51282	0.51279	0.51271
Nd(I)	2.9	5.7	8.9	9.8	8.9	11.4	4.6	4.4	12.1	4.5	7.80	7.3	5.6
Rb (ppm)	2.4	4.2	2.7	2.5	11	0.44	15	12	0.24	1.2	4.3	19	3.4
Sr (ppm)	155	68	99	92	308	44	8.3	612	89	100	43	127	190
⁸⁷ Rb/ ⁸⁶ Sr	0.04	0.18	0.08	0.08	0.10	0.03	5.16	0.05	0.01	0.03	0.283	0.424	0.050
⁸⁷ Sr/ ⁸⁶ Sr ₍₀₎	0.70467	0.70514	0.70444	0.70406	0.70430	0.70391		0.70444	0.70306				
⁸⁷ Sr/ ⁸⁶ Sr _(I)	0.70457	0.70471	0.70426	0.70387	0.70405	0.70385		0.70431	0.70304				
U (ppm)	0.15	0.16	0.29	0.29	1.2	0.09	0.18	0.11	0.16	0.24	0.19	0.44	0.60
Th (ppm)	0.61	0.64	0.41	0.20	0.43	0.23	0.69	0.29	0.26	0.37	0.54	0.13	0.12
Pb (ppm)	2.3	1.3	2.8	1.1	4.2	1.0	1.0	9.2	0.92	0.78	0.28	0.17	0.08
²⁰⁶ Pb/ ²⁰⁴ Pb ₍₀₎	18.60	19.51	18.62	18.85	18.86	18.66	18.76	18.41	18.74	19.09		18.75	18.44
²⁰⁷ Pb/ ²⁰⁴ Pb ₍₀₎	15.58	15.65	15.55	15.51	15.52	15.50	15.58	15.55	15.46	15.64		15.55	15.55
²⁰⁸ Pb/ ²⁰⁴ Pb ₍₀₎	38.34	38.92	38.14	37.93	37.97	38.01	38.35	38.09	37.81	38.56		37.96	37.36
²³⁸ U/ ²⁰⁴ Pb	4.29	8.35	6.64	16.89	18.00	5.89	11.28	0.74	10.65	19.99		24.89	8.30
²³⁵ U/ ²⁰⁴ Pb	0.03	0.06	0.05	0.12	0.13	0.04	0.08	0.01	0.08	0.15		0.18	0.06
²³² Th/ ²⁰⁴ Pb	17.84	33.67	9.72	11.93	6.69	15.99	44.61	2.03	18.74	31.33		19.63	13.18
²⁰⁶ Pb/ ²⁰⁴ Pb _(I)	18.55	19.35	18.50	18.48	18.44	18.55	18.52	18.41	18.51	18.59		18.13	18.23
²⁰⁷ Pb/ ²⁰⁴ Pb _(I)	15.63	15.69	15.60	15.55	15.54	15.55	15.62	15.57	15.50	15.61		15.51	15.54
²⁰⁸ Pb/ ²⁰⁴ Pb _(I)	38.27	38.58	38.20	37.96	38.02	37.98	37.84	38.16	37.72	38.08		37.66	37.16

Sample	95-DIAB-107c	95-DIAB-14	95-DIAB-031	95-DIAB-29	MT. Diab-1	TL-4	SFM-1	SFM-6	HPSZ	SUNOL-2038	JS-Ecg	MP-1
Sm (ppm)	3.5	2.9	4.6	2.3	4.4	1.6	7.1	5.1	2.6	0.77	5.4	3.2
Nd (ppm)	8.9	11	15	7.1	12	5.5	21	15	6.2	2.5	21	7.9
¹⁴⁷ Sm/ ¹⁴⁴ Nd	0.246	0.166	0.193	0.202	0.224	0.182	0.216	0.216	0.267	0.197	0.165	0.253
¹⁴³ Nd/ ¹⁴⁴ Nd(0)	0.51290	0.51295	0.51292	0.51303	0.51305	0.51298	0.51305	0.51321	0.51305	0.51295	0.51270	0.51307
¹⁴³ Nd/ ¹⁴⁴ Nd(I)	0.51262	0.51276	0.51271	0.51281	0.51280	0.51278	0.51281	0.51297	0.51276	0.51273	0.51251	0.51279
Nd(I)	4.0	6.7	5.6	7.5	7.4	7.0	7.7	10.7	6.6	6.1	1.8	7.2
Rb (ppm)	45	4.9	1.2	14	1.0	0.50	4.7	1.3	6.9	6.7	0.13	11
Sr (ppm)	224	219	693	221	56	21	472	225	81	279	76	92
⁸⁷ Rb/ ⁸⁶ Sr	0.567	0.063	0.005	0.178	0.053	0.066	0.028	0.016	0.243	0.098	0.005	0.324
⁸⁷ Sr/ ⁸⁶ Sr ₍₀₎												
⁸⁷ Sr/ ⁸⁶ Sr _(I)												
U (ppm)	9.9	1.7	35	0.99	107	0.60	1.7	1.9	0.75	3.9	2.0	0.85
Th (ppm)	0.29	1.4	0.58	0.23	0.36	0.42	0.37	0.29	0.2	0.13	1.0	0.16
Pb (ppm)	0.39	0.39	0.31	0.18	0.18	0.13	0.18	0.18	0.22	0.04	0.09	0.20
²⁰⁶ Pb/ ²⁰⁴ Pb ₍₀₎	18.46	18.95	18.65	18.68	20.15	18.39	18.60	18.58	18.67		18.47	
²⁰⁷ Pb/ ²⁰⁴ Pb ₍₀₎	15.60	15.61	15.59	15.57	15.88	15.61	15.50	15.52	15.65		15.56	
²⁰⁸ Pb/ ²⁰⁴ Pb ₍₀₎	38.23	38.73	38.39	38.07	39.55	38.21	38.03	37.99	38.36		38.35	
²³⁸ U/ ²⁰⁴ Pb	2.51	15.35	0.56	11.57	0.11	13.52	6.71	6.03	18.85		2.82	
²³⁵ U/ ²⁰⁴ Pb	0.02	0.11	0.00	0.08	0.00	0.10	0.05	0.04	0.14		0.02	
²³² Th/ ²⁰⁴ Pb	1.95	54.38	1.08	14.94	0.23	45.62	14.22	9.72	17.19		32.91	
²⁰⁶ Pb/ ²⁰⁴ Pb _(I)	18.40	18.56	18.64	18.39	20.15	18.05	18.43	18.42	18.20		18.40	
²⁰⁷ Pb/ ²⁰⁴ Pb _(I)	15.60	15.59	15.59	15.55	15.88	15.59	15.49	15.51	15.62		15.56	
²⁰⁸ Pb/ ²⁰⁴ Pb _(I)	38.20	37.90	38.38	37.84	39.55	37.51	37.81	37.84	38.10		37.85	

The chondrite-normalized rare earth element (REE) patterns for these high-grade tectonic blocks, high-grade coherent rocks, low-grade coherent schists, and the Coast Range ophiolite are shown in Figures 4A–4D, respectively, and Western Pacific arc tholeiite data from Jakes and Gill (1970) are shown for comparison. Most of the high-grade rocks display generally flat REE patterns, although some of these rocks show light rare earth element (LREE) depletions. The two low-grade coherent rocks of this study show slight LREE depletions similar to N-MORB. The Coast Range ophiolite sample (Mt. Diab-1, Fig. 4D) has a flat pattern ($[La/Yb]_N = 1.02$; normalized to chondrite) and a very small LREE depletion and falls entirely within the field of global arcs.

The Th/Yb versus Ta/Yb ratios of samples from this study and the Ring Mountain are plotted in Figure 5. The Th/Yb ratios range from 0.01 to 2.94, and Ta/Yb ratios range from 0.02 to 0.27 for all the aforementioned rocks. This plot shows how the compositions of basalts from normal oceanic arcs differ from those of active continental margins and alkalic oceanic arcs (Hawkesworth and Norry, 1983). The Franciscan rocks fall along a trend from N-MORB to Mariana arc in this diagram. All rocks fall in the fields of N-MORB and oceanic arc.

Twenty-five compatible and incompatible trace-element concentration patterns are shown normalized to N-MORB in Figures 6A–6D. The high-grade rocks show high Ba and Pb concentrations and high Ba/Rb, Ba/Th, U/Th,

U/Nb, and La/Nb ratios. A strong negative Nb anomaly is observed with low Ce/Pb ratios. The low-grade rocks and the Coast Range ophiolite basalt only mildly exhibit some of the typical arc-like trace-element patterns mentioned before and clearly display a different set of trace-element concentrations and ratios compared to the high-grade rocks.

The Rb-Sr and Sm-Nd isotopic systematics data are reported in Table 4. Initial ϵ_{Nd} and $^{87}Sr/^{86}Sr$ were calculated at 169 Ma, which approximates the age of crystallization of the Coast Range ophiolite (Hopson et al., 2008; Shervais et al., 2005), as well as the oldest age of metamorphism of the high-grade rocks (Anczkiewicz et al., 2004). The initial ϵ_{Nd} and $^{87}Sr/^{86}Sr$ ratios of the tectonic block

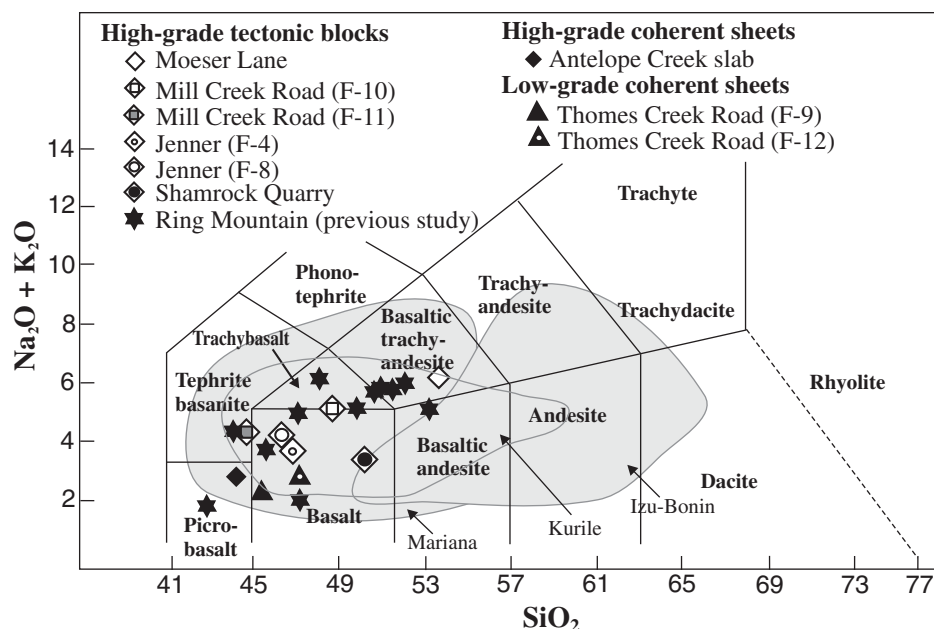


Figure 3. Na_2O and K_2O versus SiO_2 (wt%) in whole-rock samples of the Franciscan high- and low-grade blocks and coherent metamorphic rocks. These data also include our previously published results of the blueschists, eclogites, and garnet-amphibolites from Ring Mountain (RM in Fig. 1) tectonic blocks (Saha et al., 2005). Compositional ranges of volcanic rocks from the Mariana, Kurile, and Izu-Bonin intra-oceanic arcs are shown for comparison.

and coherent sheet samples of this study collected from multiple localities of the Franciscan Complex are plotted in Figure 7, along with high-grade block rocks from our previous study of the Ring Mountain area (Saha et al., 2005). Data obtained for two samples of peridotite minerals (clinopyroxenes) of the Coast Range ophiolite in a recent study (Choi et al., 2008) have also been included in this figure (Fig. 7). The initial ϵ_{Nd} values plotted in Figure 7 range from 2.9 to 9.8 for the high-grade rocks, while the two low-grade epidote blueschists have distinctly higher $\epsilon_{\text{Nd(t)}}$ values of 11.4 and 12.1. The initial $^{87}\text{Sr}/^{86}\text{Sr}$ values of the high-grade rocks range from 0.70387 to 0.70471. The low-grade rocks have distinctly lower $(^{87}\text{Sr}/^{86}\text{Sr})_i$ values of 0.70385 and 0.70304. The low-grade rocks fall in the field of MORB, and the high-grade rocks fall within or below the field of arc tholeiites. Choi et al. (2008) recently reported similar data for three Coast Range ophiolite peridotite mineral samples, where one sample fell within the field of MORB ($\epsilon_{\text{Nd(t)}} = 12.5$, $^{87}\text{Sr}/^{86}\text{Sr}_{[0]} = 0.702496$) and the other two samples were within the field of arc tholeiites, similar to the high-grade samples of this study. Choi et al. (2008) suggested that the MORB-like peridotites may be representative of a remnant oceanic lithosphere that

had preserved the mantle wedge composition prior to suprasubduction-zone modification.

Initial $^{206}\text{Pb}/^{204}\text{Pb}$, $^{207}\text{Pb}/^{204}\text{Pb}$, and $^{208}\text{Pb}/^{204}\text{Pb}$ ratios of the Franciscan rocks at 169 Ma have ranges of 18.13–20.15, 15.49–15.88, and 37.16–39.55, respectively, as reported in Table 4. Pb-Pb isotopic ratios of these rocks are plotted in Figure 8, along with high-grade rocks of the previous study by Saha et al. (2005) and Coast Range ophiolite peridotites (Choi et al., 2008), and they are compared to Pb-isotopic ratios of three intra-oceanic arcs of the Western Pacific, i.e., the Mariana, Kurile, and Izu-Bonin arcs and Pacific MORB (GEOROC database, Max Planck Institute). Various mantle reservoirs and the Northern Hemisphere reference line (NHRL) are also plotted in Figure 8 for reference. The Franciscan Pb data are similar to the Izu-Bonin and Mariana arcs (Pearce et al., 1992), even though they also fall within the field of Pacific MORB (Church and Tatsumoto, 1975; Hanan and Schilling, 1989; Tatsumoto, 1978; White et al., 1987). All these rocks show a steeper trend than the NHRL and are similar to those of the Western Pacific arc rocks. Note that the low-grade coherent schists plot closer to the NHRL (compared to all other high-grade rocks), and their Pb isotopes are similar to both Pacific MORB and Izu-Bonin arc material.

INTERPRETATION OF GEOCHEMICAL DATA

The major-element chemical compositions of the Franciscan rocks of this study (Fig. 3) are consistent with a calc-alkaline affinity for the protoliths of these metamorphic rocks. In order to assess protoliths, or rather the tectonic affinity of those protoliths, with our geochemical data, the degree to which metamorphism may have affected the geochemical signature needs to be evaluated.

The major-element compositions of these rocks are remarkably consistent despite their diverse spatial and metamorphic relations. If all these rocks had a MORB protolith, then their major-element composition started off being in the box marked as basalts in Figure 3. However, this plot indicates enrichment in Na and K and both enrichment and depletion in SiO_2 relative to the basalt field. Metasomatic processes associated with blueschist-, eclogite-, and amphibolites-facies metamorphism (Sorensen et al., 1997) and palagonitization within the top few hundred meters of the ocean floor may cause enrichment in K (Ridley et al., 1994). Na enrichment in rocks due to spilitization of the ocean floor is also common. However, the data indicate that it is also likely that the Franciscan rocks of our study were variable in Na, K, and SiO_2 , similar to rocks of calc-alkaline affinity, before alteration and metamorphism. Two samples from Panoche Pass and Mill Creek Road (Fig. 3) have lower SiO_2 than basalts. Alteration of N-MORB does not cause any SiO_2 depletion; hence, these two rocks probably had low SiO_2 in their protoliths. In the other extreme, high SiO_2 (consistent with petrographically observed free quartz) and high $\text{Na}_2\text{O} + \text{K}_2\text{O}$ are observed in the high-grade tectonic block from El Cerrito (Fig. 3). Major-element compositions are consistent with an arc tholeiite origin for samples with silica depletion. Accordingly, variability in major-element compositions of our samples may reflect protolith variability rather than element mobility during metamorphism. A more rigorous evaluation of element mobility versus protolith geochemical signatures is given later in our assessment of REE data (no exchange with continentally derived sediments) and trace-element data (different protolith signatures for rocks of same metamorphic grade). Some samples may have either seawater-altered MORB or arc tholeiites as their protolith, based on their major-element chemistry, but we can further discriminate between these alternatives on the basis of our trace element and isotopic data, as discussed in the following sections.

The REE patterns of most of the Franciscan rocks (Fig. 4) fall entirely within the field of

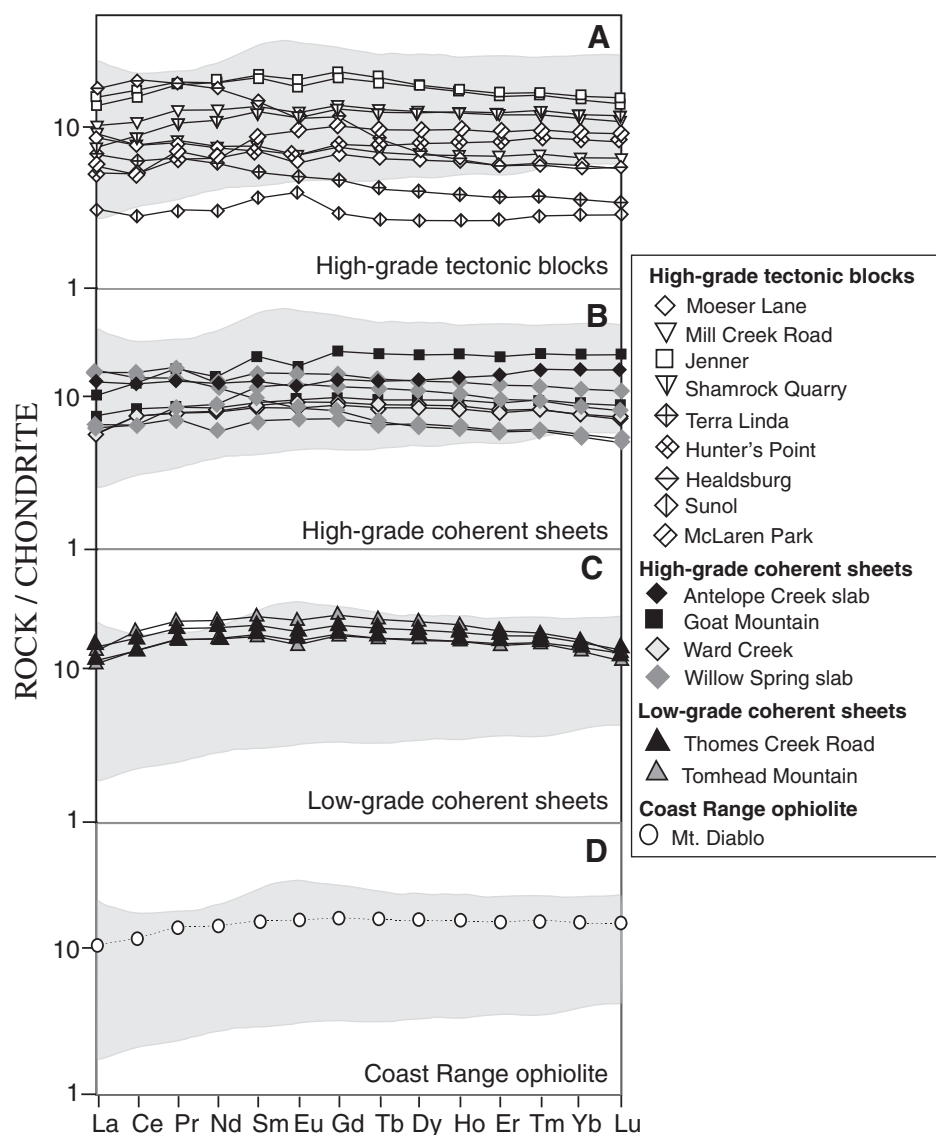


Figure 4. Chondrite-normalized rare earth element (REE) patterns of (A) high-grade tectonic blocks, (B) high-grade coherent sheets, (C) low-grade coherent sheets, and (D) Coast Range ophiolite (CRO) basalt. The high-grade and low-grade rocks and the Coast Range ophiolite basalt display similar patterns, showing slight light REE depletion analogous to South Sandwich Islands, Izu-Bonin, and Mariana arc basalts (Hawkesworth et al., 1977; Tatsumi and Eggins, 1995; Bloomer, 1987). The shaded region is a summary of Western Pacific arc tholeiite data (Jakes and Gill, 1970).

Western Pacific arc tholeiites, and their overall patterns are similar to global island-arc basalts (Hawkesworth et al., 1977; Tatsumi and Eggins, 1995). These rocks are distinctly different from OIB and enriched MORB (E-MORB), and we can conclude that either MORB or arc tholeiites could be the protoliths of these high- and low-grade rocks and the Coast Range ophiolite basalt. From our REE data (Fig. 4), which do not show perceptible LREE enrichment relative to N-MORB, we exclude the possibility of any

continental contamination from continentally derived sediments as part of the protolith or elemental exchange with such sediments during metamorphism. We can also rule out ocean-island basalts or seamounts as possible protoliths for these rocks from their REE data.

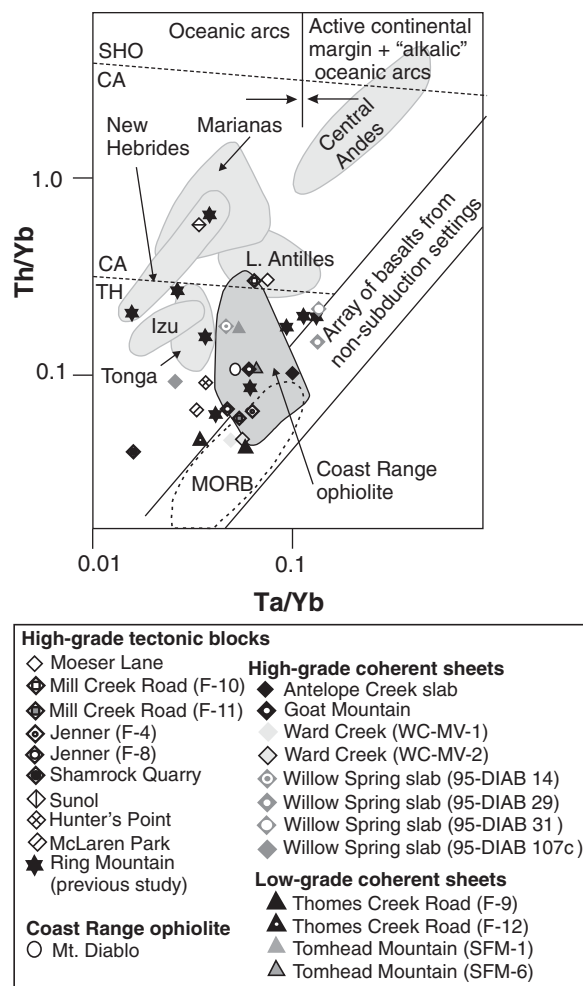
Arc-related geochemical signatures can be effectively discriminated from other mantle components in the plot of Th versus Ta (Fig. 5; both axes normalized to Yb) (Pearce et al., 1992; Giaramita et al., 1998). There is an overlap on

this diagram between island-arc tholeiites and mid-ocean-ridge basalts. However, Th is chosen over K (which gives a better discrimination between different mantle components) because it is less mobile in aqueous fluids and hence more important in the study of altered and metamorphosed rocks (Pearce et al., 1992). In this diagram, the Franciscan rocks (from the current and the previous study) define a vertical trend that extends from the field of N-MORB to the field of Mariana arc. Giaramita et al. (1998) reported similar values for a set of arc-crust samples from the Coast Range ophiolite. It is interesting to note that two of the low-grade rocks (F-9 and F-12 from Thomes Creek Road; Table 1; Fig. 5) fall within the array of basalts from nonsubduction settings, while all high-grade rocks (except Sunol-2038) fall either above the field of non-subducted basalts or within the field of Coast Range ophiolite, which has been previously established as an arc.

Multiple trace-element patterns normalized to N-MORB are shown in Figure 6. During subduction, the oceanic slab devolatilizes and dehydrates to release fluids into the overlying mantle wedge. These fluids react with the mantle wedge and form a partial melt, which ultimately gives rise to lavas with arc signatures. N-MORB-normalized trace-elements patterns characteristic of arcs have Nb-depletion, high concentrations of Ba and Pb, and high Ba/Pb, Ba/Th, U/Th, U/Nb, and La/Nb ratios. They also show low Ce/Pb ratios (Tatsumi and Eggins, 1995). All the Franciscan high-grade rocks show these characteristic arc signatures, and they have Ba and Pb concentrations that reach up to more than 100 times the average upper-crustal composition as defined by Hart and Staudigel (1989). Hence, arc tholeiites can be concluded to be the protoliths of these high-grade rocks. The typical arc-like trace-element signatures described already for the high-grade rocks of the Franciscan Complex are only partially present with less pronounced peaks in the low-grade rocks from Thomes Creek Road and Tomhead Mountain, implying a different nonarc protolith for these low-grade coherent schists. The Coast Range ophiolite basalt shows a flat pattern with high Pb concentration (almost 1000 times NMORB) and Sr depletion.

The MORB-like rocks from Tomhead Mountain of this study have experienced the same grade of metamorphism (epidote blueschist) as arc-like rocks from Ward Creek, and one of the arc-like samples from the Willow Spring slab, as well as a higher grade of metamorphism than the lowest grade arc-like sample from the Willow Springs slab (which is lawsonite blueschist). The Tomhead Mountain rocks show MORB-like trace-element patterns (Figs. 4 and 6)

Figure 5. Th/Yb versus Ta/Yb diagram showing the compositional variation of basalts in different tectonic settings. The “mantle” array, and the tholeiitic (TH), calc-alkaline (CA), and shoshonitic (SHO) boundaries for arc basalts are from Pearce (1982). Rocks from the current study and from a previous study (Saha et al., 2005) have been plotted in this diagram, and they show a strong vertical trend from normal mid-ocean-ridge basalt (N-MORB) to Mariana arc.



despite their complete metamorphic recrystallization, and we infer there was no trace-element mobilization during metamorphism of these rocks. The coherent rocks from Ward Creek and the structurally lower part of the Willow Spring slab, classified as “high-grade” on the basis of metamorphic age, show arc-like trace-element patterns and ratios (Figs. 4, 5, and 6). Since these rocks have undergone the same degree of metamorphism as the MORB-like Tomhead Mountain rocks, their arc-like signatures indicate protolith trace-element patterns and ratios, rather than being an artifact of metamorphic redistribution of elements. Stated another way, it is extremely unlikely that a subducting slab of MORB would acquire a trace-element pattern that exactly mimics that of incipient oceanic arc crust by metamorphic redistribution of elements.

In Nd-Sr isotopic space (Fig. 7), most of the high-grade rocks of this study fall within the field of arc tholeiites, and three samples show low initial ϵ_{Nd} and are below the arc tholeiitic field. The Ring Mountain high-grade Nd-Sr iso-

topic data shown by open circles (Fig. 7) have been discussed previously (Saha et al., 2005) as having an arc protolith, especially because they fall within the arc tholeiitic field. The three samples that have lower ϵ_{Nd} and fall outside the field of arc tholeiites have been explained as having nonbasaltic lithologic components such as radiolarian chert with marine Nd- and Sr- isotopic signatures. Overall, all the rocks plotted in Figure 7 can be interpreted to have had either arc tholeiite or seawater-altered MORB as their protoliths, with some marine components such as cherts, as mentioned already. It should be noted that a similar range of Nd- and Sr-isotopic data for Franciscan high-grade rocks was also reported by Nelson and DePaolo (Nelson and DePaolo, 1985). However, these authors interpreted the low ϵ_{Nd} samples as a fluid source-derived component of subducted continental sediments (Nelson, 1991, 1995).

We have already eliminated the possibility of continental crustal contamination on the basis of the REE data for the high-grade samples of this study, including the three high-grade sam-

ples with the lowest ϵ_{Nd} values (F-1, F-3, and F-11; Table 4; Fig. 7). Nd and Sr in radiolarian chert and/or in phosphatic fish teeth may have been a possible component in the subducted oceanic crust, be it MORB or nascent arc. Contamination with fossil fish teeth and/or radiolarian chert in the protolith can lower ϵ_{Nd} values and increase $^{87}\text{Sr}/^{86}\text{Sr}$ ratios, making it difficult to distinguish between seawater-altered MORB and arc tholeiites.

The two low-grade rocks from Thomes Creek Road plotted in Figure 7 and one Coast Range ophiolite sample representative of oceanic lithosphere from Choi et al. (2008) have characteristically high MORB-like ϵ_{Nd} values, and these samples plot in the field of MORB, with one sample having more radiogenic seawater-altered $^{87}\text{Sr}/^{86}\text{Sr}$. The two other low-grade rocks from Tomhead Mountain (not plotted in Fig. 7) also have high MORB-like ϵ_{Nd} values (Table 4). There is no known process that could have increased the ϵ_{Nd} values of these three rocks if they initially had an arc-like isotopic signature. Hence, rocks plotting in the field of MORB have to be of MORB origin. Thus, there is a marked distinction in the ϵ_{Nd} values between the low-grade rocks, as represented by the four samples from Thomes Creek road, Tomhead Mountain, and the Coast Range ophiolite peridotite, representing oceanic lithosphere, and all the high-grade rocks, indicating different protoliths for the high-grade and low-grade rock groups.

In the Pb-isotopic variation diagram of Figure 8, all the Franciscan rocks of this study and those of the previous study by Saha et al. (2005) show a distinct affinity with the fields of Pb-isotopic compositions of Izu-Bonin arc rocks. Arc basalts that display steep arrays in $^{207}\text{Pb}/^{204}\text{Pb}$ against $^{206}\text{Pb}/^{204}\text{Pb}$ (Fig. 8) are usually interpreted to indicate sediment involvement in their genesis (Dickens, 1995; Hawkesworth et al., 1977; Meijer, 1976). We infer that there is no contribution from continentally derived components, including sediments, as they all lie within fields of intra-oceanic arcs in Figure 8.

The MORB-like or mantle-derived Pb values in some of the high-grade blocks that fall close to the NHRL line do not rule out our hypothesis of arc tholeiites as the protoliths for these rocks, especially when we consider other trace-element concentration and ratio plots. Some nascent intra-oceanic arc basalts, such as in Izu-Bonin (Stern and Bloomer, 1992), show depleted-mantle trace-element and isotopic signatures acquired primarily from the partial melting of the mantle wedge above the subducting slab (Perfit et al., 1980; Plank and Langmuir, 1998; Stern, 1981). As we have already discussed with the REE and Sr- and Nd-isotopic data, an arc basalt origin for these Franciscan high-grade blocks is

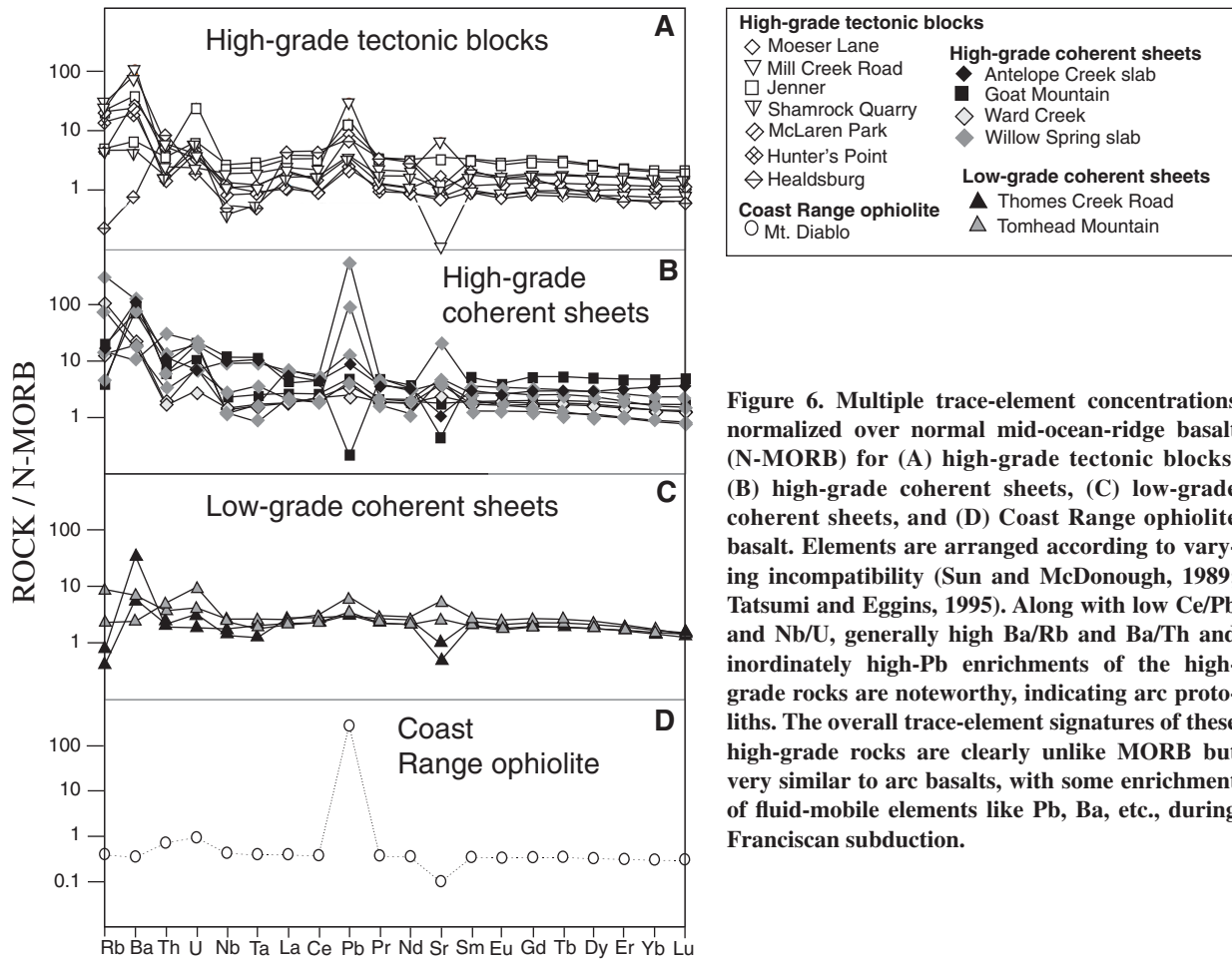


Figure 6. Multiple trace-element concentrations normalized over normal mid-ocean-ridge basalt (N-MORB) for (A) high-grade tectonic blocks, (B) high-grade coherent sheets, (C) low-grade coherent sheets, and (D) Coast Range ophiolite basalt. Elements are arranged according to varying incompatibility (Sun and McDonough, 1989; Tatsumi and Eggins, 1995). Along with low Ce/Pb and Nb/U, generally high Ba/Rb and Ba/Th and inordinately high-Pb enrichments of the high-grade rocks are noteworthy, indicating arc protoliths. The overall trace-element signatures of these high-grade rocks are clearly unlike MORB but very similar to arc basalts, with some enrichment of fluid-mobile elements like Pb, Ba, etc., during Franciscan subduction.

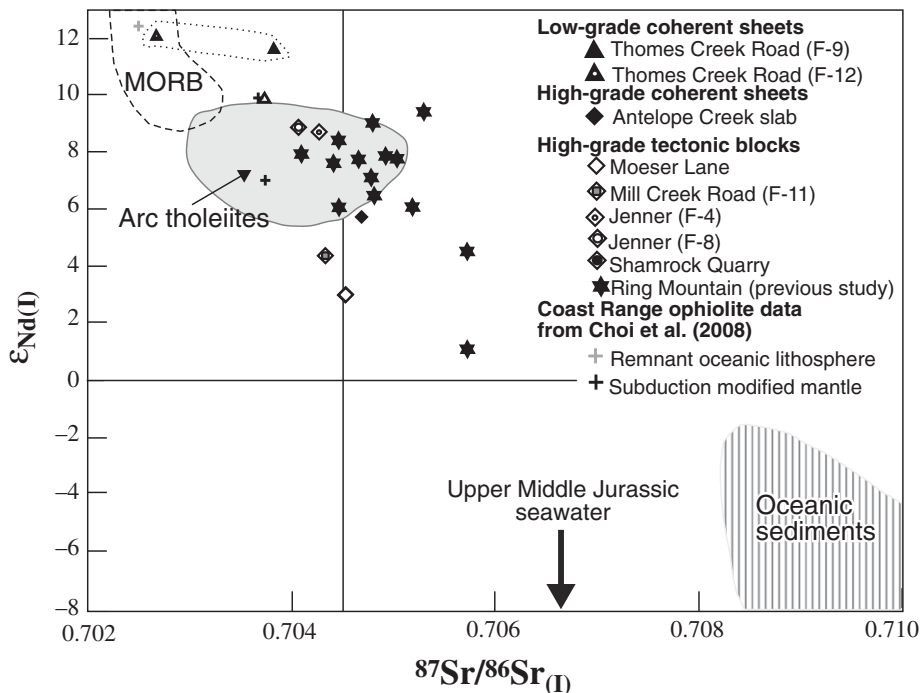


Figure 7. Initial $^{87}\text{Sr}/^{86}\text{Sr}$ and ϵ_{Nd} at 169 Ma in the Franciscan high-grade and low-grade rocks, compared with fields for present-day mid-ocean-ridge basalt (MORB), global arc tholeiites, and part of the field for oceanic sediments (Tatsumi and Eggins, 1995). All the high-grade rocks fall within or below the field of arc tholeiite and are distinctly different from the two low-grade coherent sheets, which have higher ϵ_{Nd} and fall in the field of present-day MORB.

Figure 8. Initial Pb-isotopic compositions of the Franciscan rocks at 169 Ma, compared with Pb-isotope ratios of three intra-oceanic arcs of the western Pacific. These arc data are from various sources and were by the Max Planck Data Sources (GEOROC, 2009). The Franciscan Pb data are most remarkably similar to the frontal-arc lavas of the Izu-Bonin arc (Taylor and Nesbitt, 1998). The open circles are samples from Saha et al. (2005). Other open symbols are from Choi et al. (2008). MORB—mid-ocean-ridge basalt; NHRL—Northern Hemisphere reference line; DM—Depleted mantle; EM—Enriches mantle.

indeed a viable option. Further, the Coast Range ophiolite, which is believed to have arc crust (Giaramita et al., 1998; Choi et al., 2008), and the high-grade Franciscan rocks of this study have similar Pb-isotopic values, emphasizing an arc protolith for these high-grade rocks. The four low-grade rocks of this study and the remnant oceanic lithospheric peridotite sample from Choi et al. (2008) plot closest to the NHRL and have Pb isotopes similar to both Pacific MORB and Izu-Bonin arc rocks (Fig. 8).

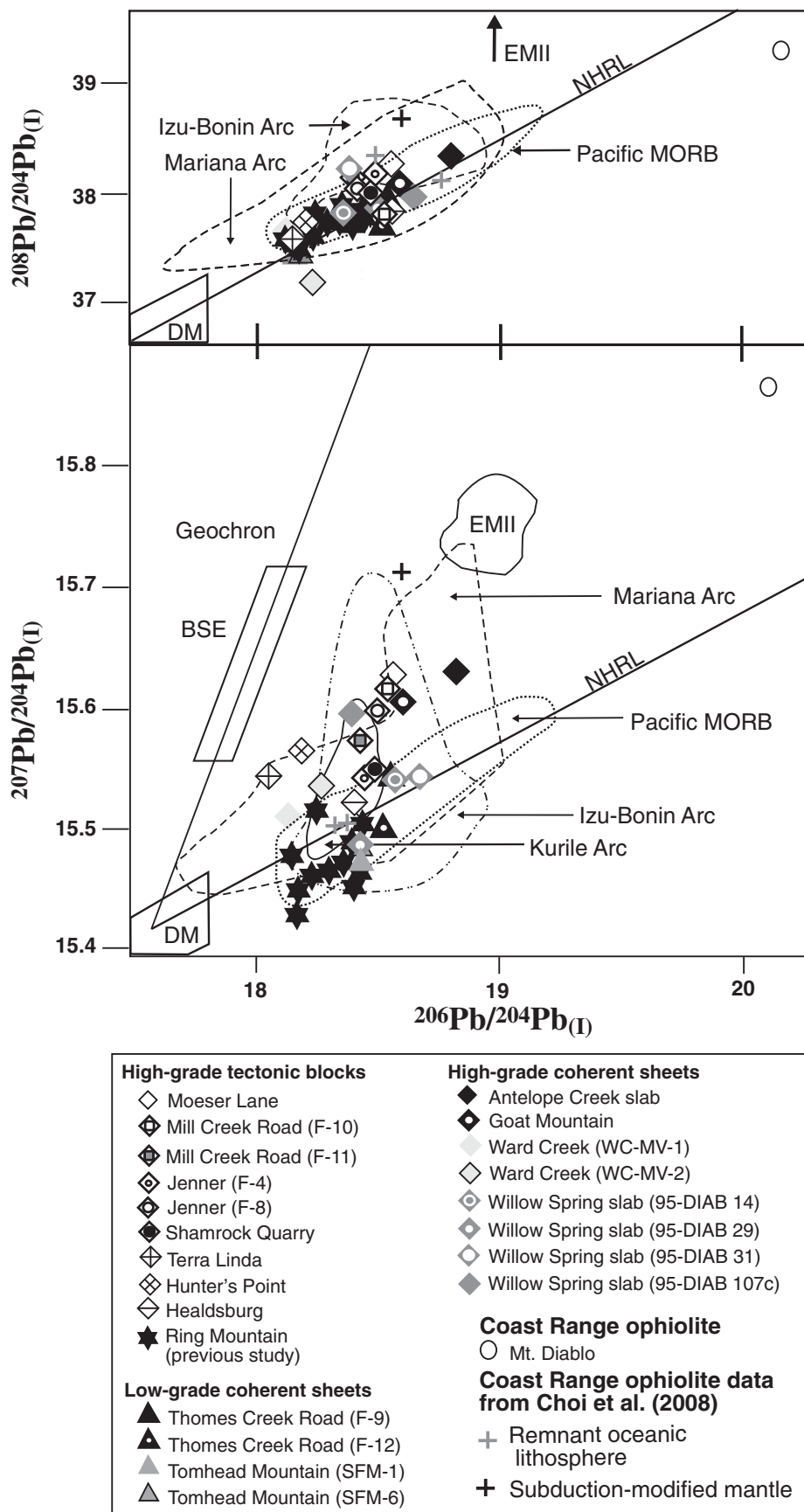
The Coast Range ophiolite basalt (Mt. Diablo-1, Table 1) falls away from all the other rocks of this study and close to the HIMU (high μ —time-integrated, high U/Pb-bearing mantle reservoirs) field (Fig. 8) and has possibly been contaminated by a HIMU source. Continental crustal contamination for this sample can be eliminated for this sample by its flat REE pattern (Fig. 4) and MORB-like trace-elemental pattern (Fig. 6).

SUMMARY FROM GEOCHEMICAL EVIDENCE

(1) Geochemical patterns observed in our metamorphic rocks reflect their protoliths and are not artifacts of element mobility during metamorphism.

(2) Major-element chemistry of the Franciscan high- and low-grade samples of our study suggests a strong calc-alkaline affinity, falling in the fields of basalt, trachybasalt, and basaltic trachyandesite (Fig. 3).

(3) There is no ocean-island basaltic or continental crustal component in the protoliths of all rocks of this study. This is clearly indicated by the REE patterns (Fig. 4) and the Pb-isotopic compositions (Fig. 8) of these rocks. Low ϵ_{Nd} in some of the samples (Fig. 8) is due to the



presence of cherts. The presence of apatite in the form of phosphatic fish teeth may also lower ϵ_{Nd} values of these rocks.

(4) Different protoliths for high- and low-grade rocks are distinguished by their isotopic compositions and by their trace-element concentrations and ratios. In Sr-Nd isotopic ratios (Fig. 7), low-grade rocks show MORB-like characteristics that are distinctly different from the high-grade rocks. Pb-isotopic ratios indicate that the high-grade rocks have a strong resemblance to Western Pacific intra-oceanic arc rocks (Fig. 8). The high-grade rocks are inferred to have an arc protolith.

(5) The geochemical signatures of some of the high-grade samples are similar to MORB. However, it is not uncommon for arc regions to contain N-MORB-like rocks in terms of their geochemical and isotopic characteristics (Caprilli and Leitch, 2002; DeBari et al., 1999; Johnson and Fryer, 1990). It is noted that the Coast Range ophiolite contains a diversity of basalts, including island arc tholeiites as well as suprasubduction zone-related MORB components (Giaramita et al., 1998; Shervais, 2001; Choi et al., 2008). Therefore, even though some high-grade samples of this study may show N-MORB-like characteristics, they do not require the protoliths of all the high-grade rocks of this study to have formed in a MORB-like setting.

(6) The protoliths of the high-grade rocks were likely arc tholeiites, similar to those in the west Pacific intra-oceanic arcs. They require an arc source, and there is no evidence of subducted ridge components in our geochemical data of the high-grade Franciscan rocks.

METAMORPHIC SOLES AND SUPRASUBDUCTION-ZONE OPHIOLITE GENERATION AND EMPLACEMENT: A TECTONIC MODEL

Coherent versus Blocks-in-Mélange: Significance for Tectonic Interpretations

Until recently, high-grade metamorphism in the Franciscan Complex has been considered to occur only in tectonic blocks-in-mélange or “high-grade blocks,” with the possible, but not widely publicized, exception of a locality at Goat Mountain that may be a series of thrust sheets (hundreds of meters in map dimension) of high-grade metamorphic rocks (Ernst et al., 1970; Suppe and Foland, 1978). Wakabayashi and Dumitru (2007) recently identified several coherent high-grade slabs, including the Willow Spring slab, which is $\sim 1.5 \times 1.5$ km in map view, and the Antelope Creek slab (previously considered a block, probably because of its high-grade metamorphism) dated by Ross and Sharp

(1988) and Anczkiewicz et al. (2004). Both slabs occur at the structurally highest level in the complex, and they structurally overlie coherent blueschist-grade Franciscan meta-graywacke along discrete low-angle fault contacts (shear zone less than 10 m thick), so they are not large blocks-in-mélange. The Ward Creek coherent locality shows “high-grade” affinity in terms of metamorphic age, given that its white mica age of 154 Ma is within the range of white mica ages from high-grade blocks and slabs (138–159 Ma) (Wakabayashi and Dumitru, 2007).

Coherent field relations of Franciscan high-grade rocks are important because such rocks cannot be emplaced into the Franciscan as olistostrome blocks, nor could they have moved in mud/serpentine diapirs; coherent Franciscan rocks must have been derived from the subducting plate. Accordingly, they share a genetic structural linkage with the rest of the Franciscan Complex and could not have been derived by exhumation and erosion from the Coast Range ophiolite or other units on the upper plate of the subduction system. Some lower-grade blocks in Franciscan mélanges exhibit suprasubduction-zone geochemistry and petrology (MacPherson et al., 1990; Erickson et al., 2004). These blocks resemble rocks of the Coast Range ophiolite (or eroded equivalent), and we interpret them as having been derived as olistostrome blocks from exhumed Coast Range ophiolite, in contrast to having been scraped off (tectonically underplated from) the downgoing plate (Fig. 9). The Saha et al. (2005) samples consisted of high-grade blocks only, and although numerous arguments have been presented tying the blocks to a Franciscan origin (scraped off of down going plate) (e.g., Platt, 1975; Cloos, 1985; Wakabayashi, 1990), derivation of such rocks from non-Franciscan sources is an alternative interpretation (e.g., Coleman and Lanphere, 1971; Moore, 1984). Although the finding of coherent sheets of Franciscan high-grade material strongly supports the model that high-grade blocks and their coherent equivalents were scraped off the downgoing plate (Wakabayashi and Dumitru, 2007), this study analyzed geochemical data from four high-grade coherent units as well as multiple high-grade block samples.

High-Grade (Metamorphic Sole) Metamorphism: Inception of Subduction or Ridge Subduction?

Field relations now confirm a subducted plate “metamorphic sole” origin for Franciscan high-grade metamorphic rocks, but two alternative models exist for high-grade Franciscan material and metamorphic soles: (1) high-grade metamorphism at the inception of subduction near a

spreading center (spreading center on what becomes upper plate) (Williams and Smyth, 1973; Platt, 1975; Cloos, 1985; Wakabayashi, 1990) and (2) subduction of an active spreading ridge after initiation of subduction (Shervais, 2001).

Both models can produce high-*T* metamorphism, account for the presence of both coherent rocks and blocks-in-mélange, and are compatible with counterclockwise *P-T* paths of high-grade metamorphism. Ridge subduction predicts high-*T*, low-*P* metamorphism (Sisson and Pavlis, 1993; Brown, 1998). The ridge subduction model, as defined by Shervais (2001), predicts subduction of a true mid-ocean-ridge spreading center, so the high-*T*, low-*P* metamorphic rocks formed by such an event should have MORB protoliths (and no suprasubduction-zone protoliths). The ridge subduction model does not require a close correspondence between the age of high-grade metamorphism (caused by ridge subduction) and the age of the suprasubduction-zone ophiolite because there is no reason why a mid-ocean-ridge spreading center should always be close to the suprasubduction-zone spreading center on the downgoing plate. The subduction initiation model predicts that metamorphic sole will be composed of high-*T*, and medium- to high- or very high-*P* rocks, and it requires the downgoing plate and the upper plate to be young (generally less than 5 m.y.) in order to achieve the temperatures of metamorphism noted in soles (Spray, 1984; Jamieson, 1986; Hacker, 1990, 1991; Hacker et al., 1996). Several protolith affinities for high-grade metamorphic rocks are compatible with the subduction initiation model. If the subduction initiated within suprasubduction-zone lithosphere, then the sole should have suprasubduction-zone protoliths. If the subduction initiated at the suprasubduction zone—older MORB interface or further away from the suprasubduction-zone spreading center within MORB lithosphere, the sole protoliths should be MORB and/or OIB and not suprasubduction zone.

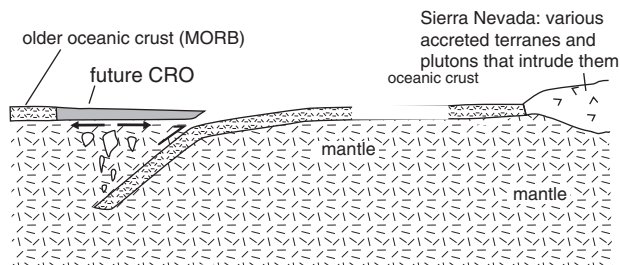
The characteristics of high-grade rocks of the Franciscan and other metamorphic soles are much more compatible with the subduction initiation, rather than the ridge subduction, model because:

(1) High-*T* Franciscan metamorphism took place at medium- to very high-*P* rather than low-*P* conditions (Wakabayashi, 1990; Anczkiewicz et al., 2004; Tsujimori et al., 2006, 2007; Page et al., 2007). Metamorphic soles elsewhere in the world exhibit high-*T* and medium- to high-*P* metamorphism, rather than high-*T* and low-*P* metamorphism (e.g., Jamieson, 1986; Encarnación et al., 1995; Gnos, 1998; Önen and Hall, 2000; Searle and Cox, 2002; Guilmette et al., 2008).

Coast Range ophiolite generation and emplacement

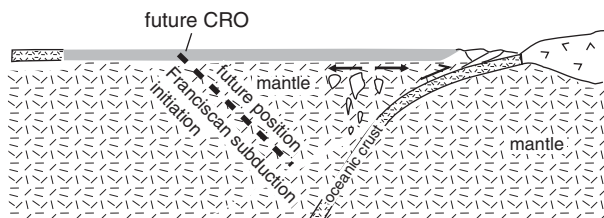
172–165 Ma (a)

Genesis of Coast Range ophiolite (CRO) in nascent arc setting



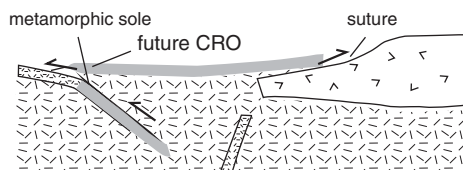
172–165 Ma (b)

terminal stages of SSZ spreading before collision



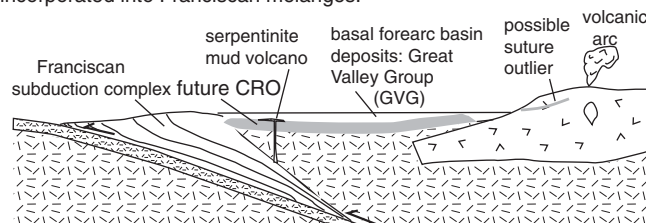
165–160 Ma

Continental margin blocks subduction zone. East-dipping Franciscan subduction initiates beneath the CRO. Metamorphic sole forms (high-grade Franciscan metamorphism) from SSZ protoliths.



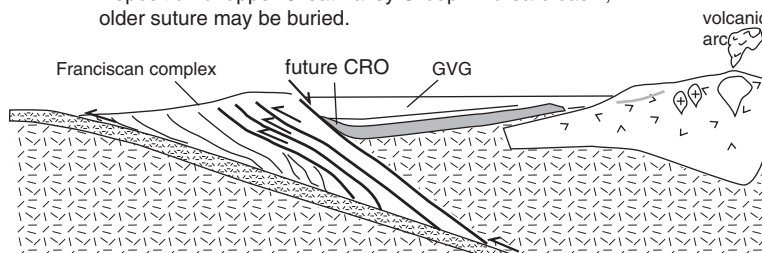
160–100 Ma

Subduction continues. Material is progressively offscraped structurally beneath sole. Sole may be largely dismembered into blocks, leaving few coherent pieces. Some exhumation of high-grade blocks may occur by serpentinite mud volcanoes. Subduction of MORB crust follows early subduction of SSZ crust. Olistostromes derived from CRO shed some (low grade) blocks of SSZ origin into Franciscan trench where they are incorporated into Franciscan melanges.



100–70 Ma

Main stage exhumation of coherent metamorphic rocks of Franciscan. Continued subduction and occasional offscraping of MORB and OIB as well as olistostromal emplacement of earlier exhumed materials. Deposition of upper Great Valley Group in forearc basin; older suture may be buried.



70–20 Ma

East-vergent tectonic wedging; continued subduction and occasional offscraping of MORB and OIB. High-grade Franciscan present structurally high as blocks and rare coherent sheets but also distributed (as blocks) to lower structural levels as a result of earlier exhumation and resedimentation to trench and reincorporation into the subduction complex.

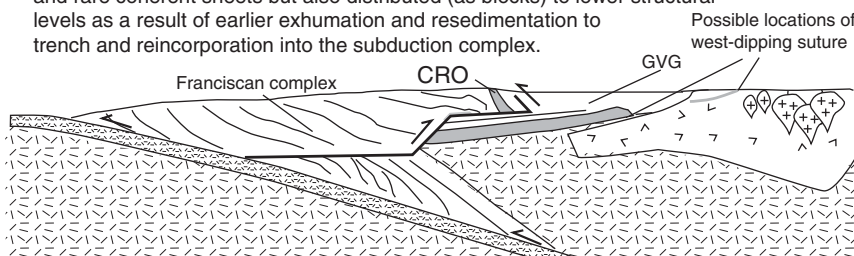


Figure 9. Tectonic model for generation and emplacement of Coast Range ophiolite and the related evolution of the Franciscan Complex. MORB—mid-ocean-ridge basalt; OIB—oceanic-island basalt; SSZ—suprasubduction zone.

(2) The ages of Franciscan high-grade metamorphism are very close to the igneous age of the overlying Coast Range ophiolite, just as ages of metamorphic soles throughout the world are close to the igneous ages of the structurally overlying ophiolites (e.g., Spray, 1984; Jamieson, 1986; Wakabayashi and Dilek, 2000).

(3) The protoliths of the earliest subducted (including high-grade) Franciscan metamorphic

rocks are suprasubduction zone. Suprasubduction-zone protoliths have been identified in a few other soles, as will be discussed later.

Alternatively, the early thermal history of the Franciscan may be permissibly interpreted to support ridge subduction. Anczkiewicz et al. (2004) suggested that garnet Lu-Hf ages from Franciscan high-grade rocks reflect metamorphic crystallization, and the positive correlation

between ages and metamorphic peak temperatures shows anomalously slow cooling of the Franciscan subduction zone in the 15 m.y. or more following the inception of subduction. The slow cooling interpreted by Anczkiewicz et al. (2004) has been challenged on the basis of very low geothermal gradients recorded by revised Franciscan eclogite *P-T* estimates (Page et al., 2007), and there are a number of Ar/Ar white

mica and hornblende ages from high-grade rocks that appear to reflect faster cooling (Wakabayashi and Dumitru, 2007). If the permissible interpretation of slow cooling is accepted, the Franciscan high-grade rock characteristics still appear inconsistent with a ridge subduction model, as noted already. Apparent slow cooling may be explained by close approach, but not subduction of a ridge crest, similar to the model proposed by Uehara and Aoya (2005) for early Sanbagawa belt metamorphism.

Can a metamorphic sole develop sometime after subduction initiation as a slab rolls back and has formed, or partly formed, a supra-subduction-zone ophiolite? This is doubtful because it would involve subduction of progressively older and colder oceanic lithosphere, resulting in refrigeration of the hanging wall immediately above the subduction zone, even though extension and mantle upwelling may be occurring further inboard of the subduction zone. Even in the event of subduction erosion resulting in the removal of hanging wall and the placement of the subducting crust against hot mantle in the hanging wall, the subducting material would be old and cool enough so that there would be insufficient heat to generate the peak temperatures recorded in metamorphic soles (Hacker, 1990, 1991; Hacker et al., 1996). Accordingly, we believe that metamorphic soles, including the high-grade rocks of the Franciscan Complex, formed at the inception of subduction.

Suprasubduction-Zone Ophiolite Formation and Emplacement: The Involvement of Multiple Subduction Zones

The identification of widespread suprasubduction-zone protolith signatures in high-grade Franciscan metamorphic rocks indicates that the high-grade metamorphism that formed at the inception of Franciscan subduction occurred in basalt protoliths that formed over a different (pre-Franciscan) subduction zone (Fig. 9). Although the pre-Franciscan subduction zone is not directly constrained to be the same one over which the Coast Range ophiolite formed, the simplest model would form both the Coast Range ophiolite and the protoliths for Franciscan high-grade rocks over the same subduction zone. That Franciscan subduction initiated near the Coast Range ophiolite spreading center is consistent with the following: (1) subduction initiation within young (<5 m.y.) oceanic lithosphere, which is necessary to attain the high temperatures of metamorphism of Franciscan high-*T* metamorphism (and the high-*T* metamorphism of metamorphic soles in general; Hacker, 1991; Hacker et al., 1996); (2) the closeness in age between Franciscan high-*T* metamorphism

and Coast Range ophiolite crystallization ages; and (3) the suprasubduction-zone character of both the Coast Range ophiolite and Franciscan high-grade metamorphic rocks.

Based on petrologic, geochemical, and geochronologic data alone, the pre-Franciscan subduction zone may have dipped either west or east, but we prefer a west-dipping subduction zone for the following reasons.

(1) There is no evidence of a pre-Franciscan subduction complex west of the Franciscan Complex. Subduction zones are commonly terminated by failed subduction of a buoyant terrane, resulting in a suture zone that itself cannot be subducted and would probably be preserved were it to be swept into a younger subduction zone (given that whatever blocked and stopped the first subduction zone would [at minimum] be accreted at the later one). It is also difficult to remove evidence of an east-dipping pre-Franciscan subduction zone by later strike-slip faulting because the older subduction-zone suture would have been located on the down-going plate during Franciscan subduction. It is difficult to envision a scenario whereby such a suture could be transported without being drawn into the subduction zone; where some parts of it should be incorporated into the Franciscan subduction complex, total subduction erosion of such material, while possible, would be comparatively unlikely. In obliquely convergent plate margins, strike-slip faults are present on the upper plate, not the downgoing plate, so removal of old subduction complex material by strike-slip faulting to distant regions is not likely (e.g., Fitch, 1972; Beck, 1983; McCaffrey, 1992) (Fig. 10).

(2) In contrast to the lack of evidence for an east-dipping pre-Franciscan subduction zone, there are at least two permissible alternatives for west-dipping sutures of the appropriate age in the western Sierra Nevada and possibly beneath the sediments of the Central Valley (Saha et al., 2005). Garnet amphibolite associated with an apparent west-dipping suture crops out structurally beneath the Jarbo Gap ophiolite in the northern Sierra Nevada, and these rocks may be the metamorphic sole to the Jarbo Gap ophiolite (Wakabayashi and Dilek, 1987). These high-grade metamorphic rocks are similar in their structural context to garnet amphibolite blocks that have yielded 178 Ma Ar/Ar hornblende ages further south in the Tuolumne Complex (Sharp and Leighton, 1987; Sharp, 1988). Thus, a west-dipping subduction zone may have initiated in what became the western Sierra at ca. 178 Ma ("possible position of west-dipping suture [daylighting]" on Fig. 2), forming the garnet amphibolites as part of a metamorphic sole, and this subduction zone may be of appropriate age to have formed the 172–165 Ma Coast Range

ophiolite (Figs. 2 and 9). Another potential suture has been located beneath the eastern margin of the Central Valley, associated with one of the most prominent magnetic anomalies in North America (Godfrey and Klemperer, 1998; Godfrey and Dilek, 2000) ("possible position of buried west-dipping suture" on Fig. 2). Potential field and seismic data indicate that a zone of ultramafic rocks dips west beneath the cover of the Great Valley Group. It is not clear whether this suture is observable in exposed basement rocks in the western Sierra Nevada or whether it is entirely buried beneath Great Valley Group sedimentary rocks. If it does reach the surface, it may be related to the suture beneath the Jarbo Gap ophiolite noted above, or it may be a separate feature.

(3) For a nascent arc environment of supra-subduction-zone ophiolite generation, there is virtually no room to place two subduction zones of the same polarity (a first subduction zone that the suprasubduction-zone ophiolite forms over and a second one that this ophiolite is emplaced over) and still have the spreading center (with the least dense lithosphere) in the hanging wall of the second subduction zone (Fig. 10). If the suprasubduction-zone ophiolite was generated in an intra-arc or back-arc setting, there is more across-strike space for creation of a second subduction zone with the same polarity as the first. The latter scenario has been proposed for generation and emplacement of the Josephine ophiolite (e.g., Harper et al., 1990), as an alternative for emplacement for Philippine ophiolites (Encarnación, 2004), and for emplacement of an ophiolite in the Yarlung-Zangbo suture (Guilmette et al., 2009).

We envision the Coast Range ophiolite as having formed at 172–165 Ma associated subduction rollback and extension of older oceanic crust (possibly MORB) over a west-dipping subduction zone that reaches the surface in the Sierra Nevada or is buried beneath the Great Valley Group as noted above (Figs. 2 and 9). A mature arc edifice may not have been formed, although some have proposed the Smartville arc of the western Sierra Nevada as such an arc (Moores, 1970; Saleeby, 1982; Dickinson et al., 1996). The west-dipping subduction was blocked by the western North American margin, which was more an amalgamation of various oceanic terranes (arc fragments, oceanic crustal sheets, basinal deposits, subduction complexes) than true continental crust. The blockage and termination of west-dipping subduction resulted in the initiation of east-dipping Franciscan subduction within suprasubduction-zone oceanic crust to the west (Fig. 9) at 169–160 Ma, beginning with Franciscan high-grade metamorphism. The upper plate of

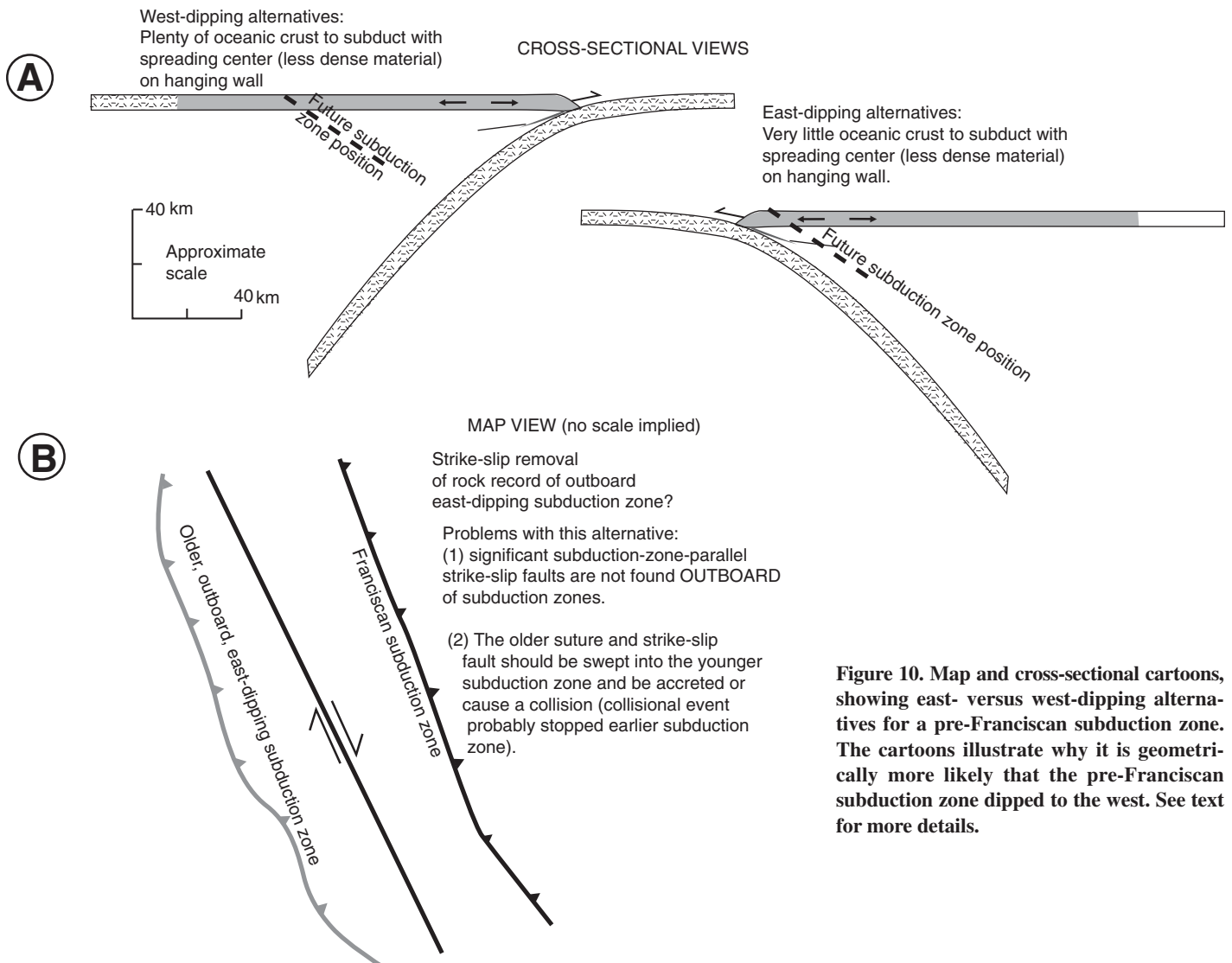


Figure 10. Map and cross-sectional cartoons, showing east- versus west-dipping alternatives for a pre-Franciscan subduction zone. The cartoons illustrate why it is geometrically more likely that the pre-Franciscan subduction zone dipped to the west. See text for more details.

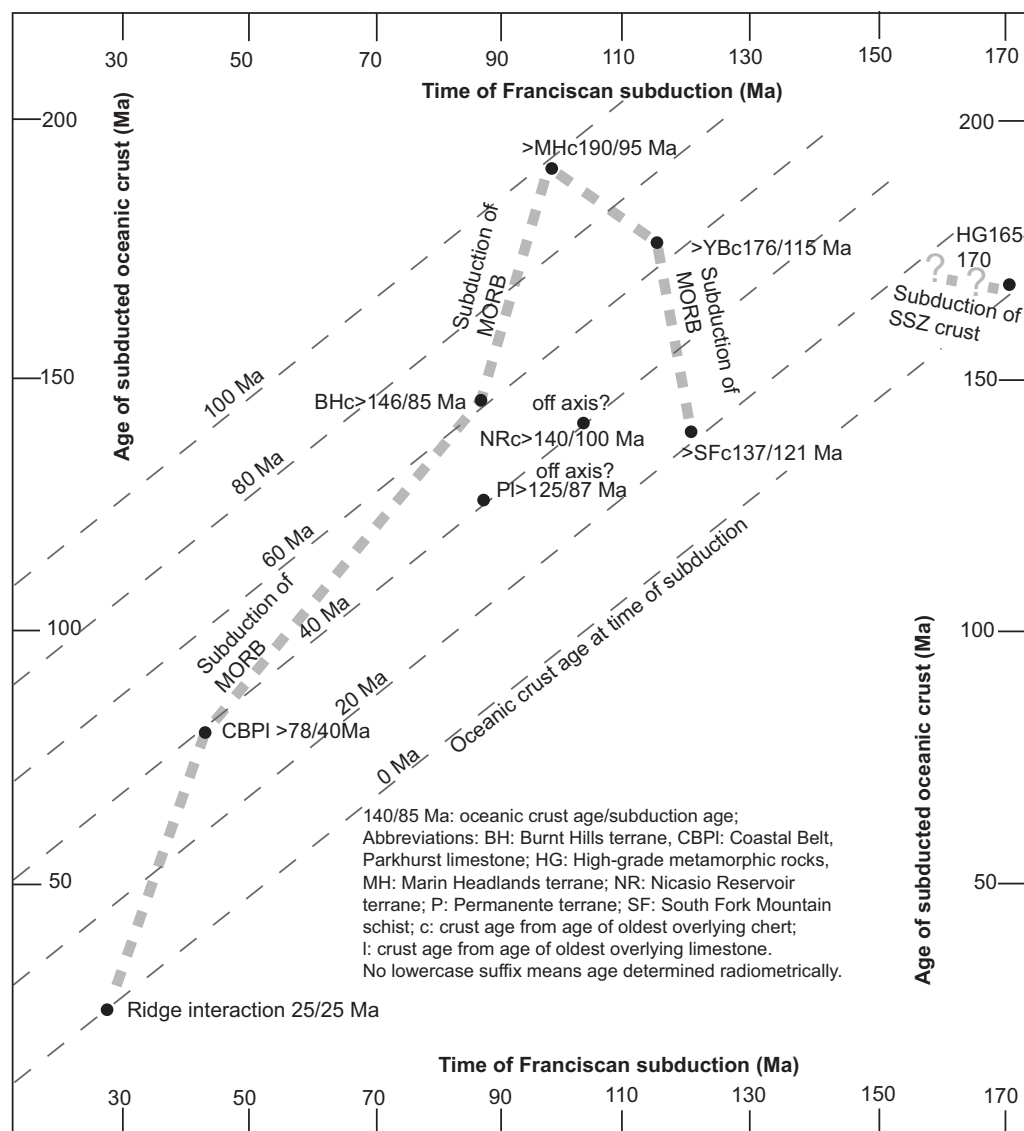
suprasubduction-zone lithosphere that did not subduct became the Coast Range ophiolite. The general model of initial west-dipping subduction followed by subduction cessation and initiation of an east-dipping Franciscan subduction has been proposed before (Moores, 1970; Schweickert and Cowan, 1975; Dickinson et al., 1996; Ingersoll and Schweickert, 1986).

Following subduction initiation, the suprasubduction-zone crust was entirely subducted, and subduction of (initially) older MORB began. The minimum duration of suprasubduction-zone subduction may be given by the ages of high-grade metamorphism (ca. 169–153 Ma), although this range may be enlarged owing to analytical uncertainties and other geochronologic issues. The maximum duration of suprasubduction zone-crust subduction may be constrained by the subduction of the MORB

South Fork Mountain schist. These rocks have yielded $^{40}\text{Ar}/^{39}\text{Ar}$ white mica ages of ca. 121 Ma (Wakabayashi and Dumitru, 2007), which may closely approximate the age of subduction (Dumitru et al., 2006). If so, the maximum duration of subduction of suprasubduction-zone crust is ~45 m.y. At the time of subduction, the South Fork mountain schist may have been ~16 m.y. old, based on the 137 Ma detrital zircon age of metachert that depositionally overlies the structurally highest mafic nappes of the schist (Dumitru et al., 2006). Evidence for the age of the subduction of oceanic crust comes from ages of radiolarian cherts that depositionally overlie some of the coherent metabasalts; the oceanic crust subducted at 115 Ma was at least 176 Ma and that subducted at 95 Ma was at least 190 Ma (Fig. 11). Subduction of progressively younger oceanic crust did not begin until after ca. 95 Ma.

By the time MORB began to subduct at the Franciscan subduction zone, the peak grade of metamorphism (of exhumed Franciscan rocks) was epidote blueschist (South Fork Mountain schist) or lower grade. In addition to subduction and occasional offscraping of MORB, OIB rocks were offscraped and incorporated into the Franciscan Complex (Shervais and Kimbrough, 1987; Shervais, 1990; MacPherson et al., 1990); it is likely that all of the OIB rocks sampled thus far in the Franciscan were subducted sometime after ca. 120 Ma based on geochronologic constraints of the various localities. Although intact (coherent) suprasubduction-zone crust was only subducted and accreted during the early stages of Franciscan subduction, blocks of suprasubduction-zone material were incorporated into the Franciscan mélanges long after subduction began. Some

Figure 11. The age of subducted oceanic crust versus time of subduction at the Franciscan trench (thick dashed gray line on diagram). Subduction ages were estimated by metamorphic age for high-grade metamorphic rocks (Anczkiewicz et al., 2004; Ross and Sharp, 1988; Wakabayashi and Dumitru, 2007), and detrital zircon chronology for others (Snow et al., 2009; Dumitru et al., 2006), except Yolla Bolly ages, which were adjusted 3 m.y. older to average between the detrital zircon age and the slightly older intrusive age of Mertz et al. (2001); some spread of Yolla Bolly ages (say 5–10 m.y.) may be expected during the time of Yolla Bolly subduction-accretion. Other ages were estimated from fossil ages (Sliter, 1984; Sliter and McGann, 1992; Murchey and Blake, 1992; Murchey and Jones, 1984) and, for the Parkhurst Limestone, fossil age, paleomagnetism, and plate-motion model (Harbert et al., 1984). Minimum oceanic crust age was determined on the basis of oldest cherts or limestone overlying basalt (Murchey and Blake, 1992; Sliter, 1984; Sliter and McGann, 1992), and the age of the crust at time of Franciscan subduction inception was estimated to be less than 5 Ma based on the heat required for high-temperature metamorphism. MORB—mid-ocean-ridge basalt; SSZ—suprasubduction zone.



of these blocks had an “upper-plate” origin, and these include rocks that resemble those of the Coast Range ophiolite (MacPherson et al., 1990; Erickson et al., 2004). Other blocks incorporated later into Franciscan mélanges include some of the high-grade metamorphic blocks (those occupying all Franciscan structural horizons except the highest one). These blocks were incorporated into mélange zones that did not form until tens of millions of years after the inception of subduction (Wakabayashi, 1992). High-grade blocks in these younger mélange zones may have been emplaced there either by a process that involved earlier exhumation, erosion, and sedimentation (olistostromes), and resubduction (Moore, 1984; Wakabayashi, 1992), or by tectonic erosion of material already accreted on the hang-

ing wall of the subduction zone (Cloos, 1985). A detailed discussion of these two hypotheses is beyond the scope of this paper.

The arc-trench system apparently received no clastic sedimentation for 20 m.y. or more following subduction inception. The oldest clastic rock in the Franciscan Complex is the Skaggs Spring schist, which has detrital zircon maximum depositional ages of ca. 144 Ma (Snow et al., 2009) and $^{40}\text{Ar}/^{39}\text{Ar}$ white mica ages of ca. 132 Ma (Wakabayashi and Dumitru, 2007). The 144 Ma detrital zircon age is similar to the detrital zircon age for the basal Great Valley Group rocks of the forearc basin (Surpless et al., 2006). Large-volume accretion of metaclastic rocks (or preservation of this accretion) in the Franciscan, however, is not recorded until ca. 120 Ma (Dumitru et al., 2006). This is con-

sistent with the lack of geochemical evidence for fluid interaction with continental sediments in the Franciscan high-grade rocks.

Suprasubduction-Zone Ophiolite Generation and Emplacement Model: Specific or General?

At present, it is difficult to evaluate whether the Franciscan–Coast Range ophiolite emplacement model presented here is representative of suprasubduction-zone ophiolites, owing to the comparative scarcity of geochemical analyses of metamorphic soles from other suprasubduction-zone ophiolites. Based on trace-element geochemistry, Guilmette et al. (2009) interpreted a suprasubduction-zone protolith from a metamorphic sole beneath a suprasubduction-zone

ophiolite in the Yarlung-Zangbo suture zone in Tibet; Encarnación (2004) suggested a suprasubduction-zone origin for the sole beneath the Dibut ophiolite in the Philippines, Pomonis et al. (2002) interpreted a suprasubduction-zone origin for the sole beneath the Koziakas ophiolite of Greece, an ophiolite made up of rocks that may have mixed origins (suprasubduction zone, MORB, OIB), and Parlak et al. (2006) proposed a dual suprasubduction zone and OIB origin for metamorphic sole rocks beneath the suprasubduction-zone Divrigi ophiolite of Turkey. Çelik and Delaloye (2006) interpreted an OIB origin for the sole of the suprasubduction-zone Beyeshir ophiolite in Turkey.

To explain the presence of the suprasubduction-zone character of the Zangbo sole, Guilmette et al. (2009) proposed a model in which suprasubduction-zone crust generated in a back-arc basin is emplaced over a second (younger) subduction zone, forming the sole. Encarnación (2004) proposed a series of subduction polarity flips with multiple periods of suprasubduction-zone ophiolite generation to explain the spatial and temporal relationships of suprasubduction-zone ophiolites and their soles in the Philippines, with the best example being the Zambales ophiolite, which formed above a west-dipping subduction zone and was emplaced over a younger east-dipping subduction zone.

The process of initiation of subduction within young suprasubduction-zone crust may have occurred (or is occurring) in several localities in the southwest Pacific within the last 10 m.y. (Harris, 2003). One example may be the Wetar thrust, along which is overthrust the southern margin of the suprasubduction zone South Banda Basin, which formed after 6 Ma (Harris, 2003).

Global data suggest that a suprasubduction-zone origin for metamorphic sole protoliths may be common but not universal. Subduction may initiate within older mid-ocean-ridge lithosphere or on the boundary between suprasubduction zone and mid-ocean-ridge lithosphere; both options would result in MORB/OIB protoliths for a metamorphic sole. A subduction initiation site on the mid-ocean-ridge–suprasubduction zone may be favored for MORB-derived metamorphic soles owing to the potential density contrast between the older mid-ocean-ridge and younger suprasubduction-zone lithosphere. Preliminary data (Basu, personal commun.) suggest both MORB and suprasubduction-zone protoliths for a metamorphic sole (probable early Triassic age) associated with the Feather River ultramafic belt, northern Sierra Nevada, California.

As reviewed already, suprasubduction-zone protoliths of metamorphic sole rocks seem to re-

quire the involvement of two subduction zones for suprasubduction-zone ophiolite generation and emplacement. A MORB or OIB metamorphic sole does not refute a single subduction-zone model, but neither does it support such a model. We believe evidence still favors a dual (or multiple) subduction-zone model over a single one for ophiolites overlying MORB/OIB soles, as argued by Wakabayashi and Dilek (2000, 2003). Although geochronology may be permissive of either model, the following argument supports a dual subduction-zone model. Initiation of subduction in young oceanic lithosphere is required for sufficient heat to generate the high-*T* metamorphism in the sole based on thermal models (e.g., Hacker, 1990). This means that some sort of spreading center on the hanging wall is probably present close to the site of subduction initiation. It is far simpler if this spreading center is indeed responsible for the formation of the suprasubduction-zone crust in the hanging wall (and is therefore a suprasubduction-zone spreading center over an earlier subduction zone), rather than it generating young MORB lithosphere very shortly before itself being re-extended by suprasubduction-zone spreading. On the other hand, the simplest scenario may not be the correct one, given the fact that the tectonic complexity exhibited by the southwest Pacific region is well beyond that considered in nearly all models of exhumed orogenic belts.

Note that spontaneous subduction initiation in older lithosphere (Stern, 2004) will probably not generate a metamorphic sole owing to insufficient heat, but it may well be associated with suprasubduction-zone oceanic crust formation as proposed. Our model constrains the evolution of ophiolites that have metamorphic soles. A single subduction-zone model for generation and emplacement of suprasubduction-zone ophiolites (e.g., Stern and Bloomer, 1992) may still apply to suprasubduction-zone ophiolites that lack metamorphic soles, whereas we believe that the dual subduction-zone model is required for suprasubduction-zone ophiolites with metamorphic soles.

ACKNOWLEDGMENTS

This research was supported by National Science Foundation grant EAR-0635767 to Basu and Wakabayashi. We thank J. Shervais, A. Zagorevski, and C. van Staal for detailed constructive reviews.

REFERENCES CITED

Anczkiewicz, R., Platt, J.P., Thirlwall, M.F., and Wakabayashi, J., 2004, Franciscan subduction off to a slow start: Evidence from high-precision Lu-Hf garnet ages on high grade-blocks: *Earth and Planetary Science Letters*, v. 225, p. 147–161, doi: 10.1016/j.epsl.2004.06.003.

Bailey, E.H., Irwin, W.P., and Jones, D.L., 1964, Franciscan and related rocks and their significance in the geology of western California: California Division of Mines and Geology Bulletin, v. 83, 177 p.

Basu, A.R., Sharma, M., and DeCelles, P.G., 1990, Nd–Sr isotopic provenance and trace element geochemistry of Amazonian foreland basin fluvial sands, Bolivia and Peru; implications for ensialic Andean orogeny: *Earth and Planetary Science Letters*, v. 100, no. 1–3, p. 1–17, doi: 10.1016/0012-821X(90)90172-T.

Beck, M.E., Jr., 1983, On the mechanism of tectonic transport in zones of oblique subduction: *Tectonophysics*, v. 93, p. 1–11, doi: 10.1016/0040-1951(83)90230-5.

Blake, M.C., Jayko, A.S., McLaughlin, R.J., and Underwood, M.B., 1988, Metamorphic and tectonic evolution of the Franciscan Complex, northern California, in Ernst, W.G., ed., *Metamorphism and Crustal Evolution of the Western United States: Rubey Volume*, Englewood Cliffs, New Jersey, Prentice-Hall, p. 1035–1060.

Bloomer, S.H., 1987, Geochemical characteristics of boninite and tholeiite-series volcanic rocks from the Mariana forearc and the role of an incompatible element-enriched fluid in arc petrogenesis: *Geological Society of America Special Paper*, v. 215, p. 151–164.

Brown, M., 1998, Ridge-trench interactions and high-*T*–low-*P* metamorphism, with particular reference to the Cretaceous evolution of the Japanese Islands, in Treloar, P.J., and O'Brien, P.J., eds., *What Drives Metamorphism and Metamorphic Relations?*: London, Geological Society of London, p. 137–169.

Caprarello, G., and Leitch, E.C., 2002, MORB-like rocks in a Palaeozoic convergent margin setting, northeast New South Wales: *Australian Journal of Earth Sciences*, v. 49, p. 367–374.

Çelik, Ö.F., and Delaloye, M.F., 2006, Characteristics of ophiolite-related metamorphic rocks in the Beyşehir ophiolitic mélange (Central Taurides, Turkey), deduced from whole rock and mineral chemistry: *Journal of Asian Earth Sciences*, v. 26, p. 461–476, doi: 10.1016/j.jseas.2004.10.008.

Choi, S.H., Mukasa, S.B., and Shervais, J.W., 2008, Initiation of Franciscan subduction along a large-offset fracture zone: Evidence from mantle peridotites, Stonyford: *California Geology*, v. 36, no. 8, p. 595–598.

Church, S.E., and Tatsumoto, M., 1975, Lead isotope relations in oceanic ridge basalts from the Juan de Fuca–Gorda Ridge area, N.E. Pacific Ocean: *Contributions to Mineralogy and Petrology*, v. 53, p. 253–279, doi: 10.1007/BF00382443.

Cloos, M., 1985, Thermal evolution of convergent plate-margins: Thermal modeling and re-evaluation of isotopic Ar-ages for blueschists in the Franciscan Complex of California: *Tectonics*, v. 4, p. 421–433, doi: 10.1029/TC004i005p00421.

Coleman, R.G., and Lanphere, M.A., 1971, Distribution and age of high-grade blueschists, associated eclogites, and amphibolites from Oregon and California: *Geological Society of America Bulletin*, v. 82, p. 2397–2412, doi: 10.1130/0016-7606(1971)82[2397:DAOHB]2.0.CO;2.

DeBari, S.M., Taylor, B., Spencer, K., and Fujioka, K., 1999, A trapped Philippine Sea plate origin for MORB from the inner slope of the Izu-Bonin Trench: *Earth and Planetary Science Letters*, v. 174, no. 1–2, p. 183–197, doi: 10.1016/S0012-821X(99)00252-6.

Dickins, A.P., 1995, *Radiogenic Isotope Geology*: Cambridge, Cambridge University Press, 452 p.

Dickinson, W.R., 1970, Relations of andesites, granites and derivative sandstones to arc-trench tectonics: *Reviews of Geophysics and Space Physics*, v. 8, p. 813–860, doi: 10.1029/RG008i004p0813.

Dickinson, W.R., Schweickert, R.A., and Ingersoll, R.D., 1996, Coast Range ophiolite as backarc/interarc basin lithosphere: *GSA Today*, v. 6, no. 2, p. 2–3.

Dilek, Y., 2003, Ophiolite concept and its evolution, in Dilek, Y., and Newcomb, S., eds., *Ophiolites concept and the evolution of geological thought*: Geological Society of America Special Paper 373, p. 1–16.

Dilek, Y., and Flower, M.F.J., 2003, Arc-trench rollback and forearc accretion: 2. A model template for ophiolites in Albania, Cyprus, and Oman, in Dilek, Y., and Robinson, P.T., eds., *Ophiolites in Earth History*: Geological Society of London Special Publication 218, p. 43–68.

- Dumitru, T.A., Wright, J.E., Wakabayashi, J., and Wooden, J.L., 2006, Geochronology of the Franciscan Eastern Belt in the Yolla Bolly area, northern California, and the nature of the South Fork Mountain schist: *Eos* (Transactions, American Geophysical Union), v. 87, no. 52, Fall Meeting supplement, abstract T11D-0469.
- Encarnación, J., 2004, Multiple ophiolite generation preserved in the northern Philippines and the growth of an island arc complex: *Tectonophysics*, v. 392, p. 103–130, doi: 10.1016/j.tecto.2004.04.010.
- Encarnación, J.P., Essene, E.J., Mukasa, S.B., and Hall, C., 1995, High-pressure and temperature subophiolitic kyanite garnet amphibolites generated during initiation of mid-Tertiary subduction, Palawan, Philippines: *Journal of Petrology*, v. 36, p. 1481–1503.
- Erickson, R.C., Mattinson, J., Dumitru, T.A., and Sharp, W.D., 2004, Petrology, isotope geochemistry, and geochronology of a multiply-metamorphosed granitoid exotic block in a Franciscan olistostrome mélange, Cazadero, California: *Geological Society of America Abstracts with Programs*, v. 36, no. 4, p. 39.
- Ernst, W.G., 1970, Tectonic contact between the Franciscan mélange and the Great Valley Sequence, crustal expression of a late Mesozoic Benioff zone: *Journal of Geophysical Research*, v. 75, p. 886–902, doi: 10.1029/JB075i005p00886.
- Ernst, W.G., 1971a, Do mineral parageneses reflect unusually high pressure conditions of Franciscan metamorphism?: *American Journal of Science*, v. 270, no. 2, p. 81–108.
- Ernst, W.G., 1971b, Metamorphic zonations on presumably subducted lithospheric plates from Japan, California, and the Alps: Contributions to Mineralogy and Petrology, v. 34, p. 43–59, doi: 10.1007/BF00376030.
- Ernst, W.G., 1984, Californian blueschists, subduction, and the significance of tectonostratigraphic terrains: *Geology*, v. 12, p. 436–440, doi: 10.1130/0091-7613(1984)12<436:CSATS>2.0.CO;2.
- Ernst, W.G., 1988, Tectonic history of subduction zones inferred from retrograde blueschist *P-T* paths: *Geology*, v. 16, no. 12, p. 1081–1084, doi: 10.1130/0091-7613(1988)016<1081:THOSZI>2.3.CO;2.
- Ernst, W.G., 1993, Metamorphism of Franciscan tectonostratigraphic assemblage, Pacheco Pass area, east-central Diablo Range, California Coast Ranges: *Geological Society of America Bulletin*, v. 105, p. 618–636.
- Ernst, W.G., Seki, Y., Onuki, H., and Gilbert, M.C., 1970, Comparative study of low-grade metamorphism in the California Coast Ranges and the outer metamorphic belt of Japan: *Geological Society of America Memoir* 124.
- Fitch, T.J., 1972, Plate convergence, transcurrent faults and internal deformation adjacent to Southeast Asia and the western Pacific: *Journal of Geophysical Research*, v. 77, p. 4432–4461, doi: 10.1029/JB077i023p04432.
- GEOROC database, 2009, GEOROC database: <http://georoc.mpch-mainz.gwdg.de/Entry.html> (accessed January 2009).
- Giarmita, M.J., MacPherson, G.J., and Phipps, S.P., 1998, Petrologically diverse basalts from a fossil oceanic forearc in California: The Llanada and Black Mountain remnants of the Coast Range ophiolite: *Geological Society of America Bulletin*, v. 110, p. 553–571, doi: 10.1130/0016-7606(1998)110<0553:PDBFAF>2.3.CO;2.
- Gnos, E., 1998, Peak metamorphic conditions of garnet amphibolites beneath the Semail ophiolite: Implications for an inverted pressure gradient: *International Geology Review*, v. 40, p. 281–304, doi: 10.1080/00206819809465210.
- Godfrey, N.J., and Dilek, Y., 2000, Mesozoic assimilation of oceanic crust and island arc into the North American continental margin in California and Nevada: Insights from geophysical data, in Dilek, Y., Moores, E.M., Elthorn, D., and Nicolas, A., eds., *Ophiolites and Oceanic Crust: New Insights from Field Studies and Ocean Drilling: Geological Society of America Special Paper* 349, p. 365–382.
- Godfrey, N.J., and Klempere, S.L., 1998, Ophiolitic basement to a forearc basin and implications for continental growth: The Coast Range/Great Valley ophiolite: *Tectonics*, v. 17, p. 558–570, doi: 10.1029/98TC01536.
- Guilmette, C., Hébert, R., Dupuis, C., Wang, C., and Li, Z., 2008, Metamorphic history and geodynamic significance of high-grade metabasites from the ophiolitic mélange beneath the Yarlung Zangbo ophiolites, Xigaze area, Tibet: *Journal of Asian Earth Sciences*, v. 32, p. 423–437.
- Guilmette, C., Hébert, R., Wang, C.S., and Villeneuve, 2009, Geochemistry and geochronology of the metamorphic sole underlying the Xigaze ophiolite, Yarlung Zangbo suture zone, south Tibet: *Lithos*, v. 112, p. 149–162.
- Hacker, B.R., 1990, Simulation of the metamorphic and deformational history of the metamorphic sole of the Oman ophiolite: *Journal of Geophysical Research*, v. 95, p. 4895–4907, doi: 10.1029/JB095iB04p04895.
- Hacker, B.R., 1991, The role of deformation in the formation of metamorphic gradients: Ridge subduction beneath the Oman ophiolite: *Tectonics*, v. 10, no. 2, p. 455–473, doi: 10.1029/90TC02779.
- Hacker, B.R., Mosenfelder, J.L., and Gnos, E., 1996, Rapid emplacement of the Oman ophiolite: Thermal and geochronologic constraints: *Tectonics*, v. 15, p. 1230–1247, doi: 10.1029/96TC01973.
- Hamilton, W.B., 1969, Mesozoic California and underflow of the Pacific mantle: *Geological Society of America Bulletin*, v. 80, p. 2409–2430, doi: 10.1130/0016-7606(1969)80[2409:MCATUO]2.0.CO;2.
- Hanan, B.B., and Schilling, J.-G., 1989, Easter microplate evolution: Pb isotope evidence: *Journal of Geophysical Research*, v. 94, p. 7432–7448, doi: 10.1029/JB094iB06p07432.
- Harbert, W.P., McLaughlin, R.J., and Sliter, W.V., 1984, Paleomagnetic and tectonic interpretation of the Parkhurst Ridge limestone, Coastal Belt Franciscan, northern California, in Blake, M.C., Jr., ed., *Franciscan Geology of Northern California: Pacific Section, Society of Economic Paleontologists and Mineralogists*, v. 43, p. 175–184.
- Harper, G.D., Grady, K., and Wakabayashi, J., 1990, A structural study of a metamorphic sole beneath the Josephine ophiolite, western Klamath terrane, California-Oregon, in Harwood, D.S., and Miller, M.M., eds., *Paleozoic and early Mesozoic paleogeographic relations: Sierra Nevada, Klamath Mountains, and related terranes: Geological Society of America Special Paper* 255, p. 379–396.
- Harris, R., 2003, Geodynamic patterns of ophiolites and marginal basins in the Indonesian and New Guinea regions, in Dilek, Y., and Robinson, P.T., eds., *Ophiolites in Earth History: Geological Society of London Special Publication* 218, p. 481–505.
- Hart, S.R., and Staudigel, H., 1989, Isotopic characterization and identification of recycled components, in Hart, S.R., and Gulen, L., eds., *Crust Mantle Recycling at Convergence Zones: Dordrecht-Boston, D. Reidel Publishing Company*, p. 15–28.
- Hawkesworth, C.J., and Norry, M.J., 1983, Continental Basalts and Mantle Xenoliths: Nantwich, UK, Shiva Publishing Limited, 272 p.
- Hawkesworth, C.J., O'Nions, R.K., Pankhurst, R.J., Hamilton, P.J., and Evensen, N.M., 1977, A geochemical study of island-arc and back-arc tholeiites from the Scotia sea: *Earth and Planetary Science Letters*, v. 36, p. 253–262, doi: 10.1016/0012-821X(77)90207-2.
- Hopson, C.A., Mattinson, J.M., and Pessagno, E.A., Jr., 1981, Coast Range ophiolite, western California, in Ernst, W.G., ed., *Geotectonic Development of California: Englewood Cliffs, New Jersey, Prentice-Hall*, p. 418–510.
- Hopson, C.A., Mattinson, J.M., Pessagno, E.A., Jr., and Luyendyk, B.P., 2008, California Coast Range ophiolite: Composite Middle and Late Jurassic oceanic lithosphere, in Wright, J.E., and Shervais, J.W., eds., *Ophiolites, Arcs, and Batholiths: A Tribute to Cliff Hopson: Geological Society of America Special Paper* 438, p. 1–101.
- Hsü, K.J., 1968, Principles of mélanges and their bearing on the Franciscan-Knoxville paradox: *Geological Society of America Bulletin*, v. 79, p. 1063–1074.
- Ingersoll, R.V., and Schweickert, R.A., 1986, A plate-tectonic model for late Jurassic ophiolite genesis, Nevada orogeny and forearc initiation, northern California: *Tectonics*, v. 5, p. 901–912.
- Jacobson, S.B., and Wasserburg, G.J., 1984, Sm-Nd isotopic evolution of chondrites and achondrites, II: *Earth and Planetary Science Letters*, v. 62, p. 137–150.
- Jakes, P., and Gill, J., 1970, Rare earth elements and the island arc tholeiitic series: *Earth and Planetary Science Letters*, v. 9, p. 17–28, doi: 10.1016/0012-821X(70)90018-X.
- Jamieson, R.A., 1986, P-T paths from high temperature shear zones beneath ophiolites: *Journal of Metamorphic Geology*, v. 4, p. 3–22.
- Johnson, L.E., and Fryer, P., 1990, The first evidence for MORB-like lavas from the outer Mariana forearc: Geochemistry, petrography and tectonic implications: *Earth and Planetary Science Letters*, v. 100, no. 1–3, p. 304–316, doi: 10.1016/0012-821X(90)90193-2.
- Krogh, E.J., Oh, C.W., and Liou, J.G., 1994, Polyphase and anticlockwise *P-T* evolution for Franciscan eclogites and blueschists from Jenner, California, USA: *Journal of Metamorphic Geology*, v. 12, p. 121–134, doi: 10.1111/j.1525-1314.1994.tb00008.x.
- Lissenberg, C.J., van Staal, C.R., Bédard, J.H., and Zagorevski, A., 2005, Geochemical constraints on the origin of the Annieopsquotch ophiolite belt, Newfoundland Appalachians: *Geological Society of America Bulletin*, v. 117, p. 1413–1426, doi: 10.1130/B25731.1.
- MacPherson, G.J., 1983, The Snow Mountain complex: An on-land seamount in the Franciscan terrain, California: *The Journal of Geology*, v. 91, p. 73–92, doi: 10.1086/628745.
- MacPherson, G.J., Phipps, S.P., and Grossman, J.N., 1990, Diverse sources for igneous blocks in Franciscan mélanges, California Coast Ranges: *The Journal of Geology*, v. 98, p. 845–862, doi: 10.1086/629457.
- Maruyama, S., and Liou, J.G., 1988, Petrology of Franciscan metabasites along the jadeite-glaucophane type facies series, Cazadero, California: *Journal of Petrology*, v. 29, p. 1–37.
- Maruyama, S., Liou, J.G., and Sasakura, Y., 1985, Low-temperature recrystallization of Franciscan greuwacks from Pacheco Pass, California: *Mineralogical Magazine*, v. 49, p. 345–355, doi: 10.1180/minmag.1985.049.352.05.
- McCaffrey, R., 1992, Oblique plate convergence, slip vectors, and forearc deformation: *Journal of Geophysical Research*, v. 97, p. 8905–8915, doi: 10.1029/92JB00483.
- Meijer, A., 1976, Pb and Sr isotopic data bearing on the origin of volcanic rocks from the Mariana island-arc system: *Geological Society of America Bulletin*, v. 87, p. 1358–1369, doi: 10.1130/0016-7606(1976)87<1358:PASIDB>2.0.CO;2.
- Mertz, D.F., Weinrich, A.J., Sharp, W.D., and Renne, P.R., 2001, Alkaline intrusions in a near-trench setting, Franciscan Complex, California: Constraints from geochemistry, petrology, and ⁴⁰Ar/³⁹Ar chronology: *American Journal of Science*, v. 301, p. 877–911, doi: 10.2475/ajs.301.10.877.
- Moore, D.E., 1984, Metamorphic history of a high-grade blueschist exotic block from the Franciscan Complex, California: *Journal of Petrology*, v. 25, no. 1, p. 126–150.
- Moore, D.E., and Blake, M.C., Jr., 1989, New evidence for polyphase metamorphism of glaucophane schist and eclogite exotic blocks in the Franciscan Complex, California and Oregon: *Journal of Metamorphic Geology*, v. 7, no. 2, p. 211–228, doi: 10.1111/j.1525-1314.1989.tb00585.x.
- Moores, E., 1970, Ultramafics and orogeny, with models of the US Cordillera and the Tethys: *Nature*, v. 228, no. 5274, p. 837–842, doi: 10.1038/228837a0.
- Murphy, B.M., and Blake, M.C., Jr., 1992, Evidence for subduction of a major ocean plate along the California margin during the middle to early Late Jurassic, in Dunn, G., and McDougall, K., eds., *Mesozoic Paleogeography of the Western United States—II: Pacific Section Society, Economic Paleontologists and Mineralogists*, v. 71, p. 1–18.
- Murphy, B.M., and Jones, D.L., 1984, Age and significance of chert in the Franciscan Complex, San Francisco Bay region, in Blake, M.C., Jr., ed., *Franciscan Geology of Northern California: Pacific Section, Society of Economic Paleontologists and Mineralogists*, v. 43, p. 51–70.
- Nelson, B.K., 1991, Sediment-derived fluids in subduction zones: Isotopic evidence from veins in blueschist and

- eclogite of the Franciscan Complex, California: *Geology*, v. 19, no. 10, p. 1033–1036, doi: 10.1130/0091-7613(1991)019<1033:SDFISZ>2.3.CO;2.
- Nelson, B.K., 1995, Fluid flow in subduction zones: Evidence from Nd- and Sr-isotope variations in metabasalts of the Franciscan Complex, California: *Contributions to Mineralogy and Petrology*, v. 119, no. 2–3, p. 247–262, doi: 10.1007/BF00307285.
- Nelson, B.K., and DePaolo, D.J., 1985, Isotopic investigation of metamorphism in subduction zones: The Franciscan Complex, California: *Geological Society of America Abstracts with Programs*, v. 17, no. 7, p. 674–675.
- Önen, A.P., and Hall, R., 2000, Sub-ophiolite metamorphic rocks from NW Anatolia, Turkey: *Journal of Metamorphic Geology*, v. 18, p. 483–495, doi: 10.1046/j.1525-1314.2000.00276.x.
- Page, F.Z., Armstrong, L.S., Essene, E.J., and Mukasa, S.B., 2007, Prograde and retrograde history of the Junction School eclogite, California, and an evaluation of garnet-phengite-clinopyroxene thermobarometry: *Contributions of Mineralogy and Petrology*, v. 153, p. 533–555.
- Parlak, O., Yilmaz, H., and Boztug, D., 2006, Origin and tectonic significance of the metamorphic sole and isolated dykes of the Divrigi ophiolite (Sivas, Turkey): Evidence for slab break-off prior to ophiolite emplacement: *Turkish Journal of Earth Sciences*, v. 15, p. 25–45.
- Pearce, J.A., 1982, Trace element characteristics of lavas from destructive plate boundaries, in Thorpe, R.S., ed., *Orogenic andesites*: Chichester, Wiley, p. 528–548.
- Pearce, J.A., Lippard, S.J., and Roberts, S., 1984, Characteristics and tectonic significance of supra-subduction zone ophiolites, in Kokelaar, B.P., and Howells, M.F., eds., *Marginal basin geology: Volcanic and associated sedimentary and tectonic processes in modern and ancient marginal basins*: Geological Society of London Special Publication 16, p. 74–94.
- Pearce, J.A., Thirlwall, M.F., Ingram, G., Murton, B.J., Arculus, R.J., and van der Laan, S.R., 1992, Isotopic evidence for the origin of boninites and related rocks drilled in the Izu-Bonin (Ogasawara) forearc, Leg 125, in Dearnont, L.H., Mazzullo, E.K., Stewart, N.J., and Winkler, W.R., *Proceedings of the Ocean Drilling Program, Bonin Mariana region; covering Leg 125 of the cruises of the Drilling Vessel JOIDES Resolution, Apra Harbor, Guam, to Tokyo, Japan, sites 778–786, 15 February 1989–17 April 1989*: College Stations, Texas, Ocean Drilling Program, p. 237–261.
- Perfit, M.R., Gust, D.A., Bence, A.E., Arculus, R.J., and Taylor, S.R., 1980, Chemical characteristics of island arc basalts: Implications for mantle sources: *Chemical Geology*, v. 30, p. 227–256.
- PETDB database, 2009: PETDB database: <http://petdb.ldeo.columbia.edu/petdb/> (accessed January 2009).
- Plank, T., and Langmuir, C.H., 1998, The chemical composition of subducting sediment and its consequences for the crust and mantle: *Chemical Geology*, v. 145, p. 325–394, doi: 10.1016/S0009-2541(97)00150-2.
- Platt, J.P., 1975, Metamorphic and deformational processes in the Franciscan Complex, California: Some insights from the Catalina schist terrane: *Geological Society of America Bulletin*, v. 86, p. 1337–1347, doi: 10.1130/0016-7606(1975)86<1337:MADPIT>2.0.CO;2.
- Pomonis, P., Tsikouras, B., and Hatzipanagiotou, K., 2002, Origin, evolution, and radiometric dating of sub-ophiolitic metamorphic rocks from the Koziaas ophiolite (W. Thessaly, Greece): *Neues Jahrbuch für Mineralogie-Abhandlungen*, v. 177, p. 255–276, doi: 10.1127/0077-7757/2002/0177-0255.
- Ridley, W.I., Perfit, M.R., Jonasson, I.R., and Smith, M.F., 1994, Hydrothermal alteration in oceanic ridge volcanic: A detailed study at the Galapagos fossil hydrothermal field: *Geochimica et Cosmochimica Acta*, v. 58, no. 11, p. 2477–2494, doi: 10.1016/0016-7037(94)90025-6.
- Ross, J.A., and Sharp, W.D., 1988, The effects of sub-blocking temperature metamorphism on the K/Ar systematics of hornblends: $^{40}\text{Ar}/^{39}\text{Ar}$ dating of polymetamorphic garnet amphibolite from the Franciscan Complex, California: *Contributions to Mineralogy and Petrology*, v. 100, p. 213–221, doi: 10.1007/BF00373587.
- Saha, A., Basu, A.R., Wakabayashi, J., and Wortman, G.L., 2005, Geochemical evidence for subducted nascent arc from Franciscan high-grade tectonic blocks: *Geological Society of America Bulletin*, v. 117, p. 1318–1335, doi: 10.1130/B25593.1.
- Saleeby, J.B., 1982, Polygenetic ophiolite belt of the California Sierra Nevada: Geochronological and tectonostratigraphic development: *Journal of Geophysical Research*, v. 87, p. 1803–1824.
- Schweickert, R.A., and Cowan, D.S., 1975, Early Mesozoic tectonic evolution of the western Sierra Nevada, California: *Geological Society of America Bulletin*, v. 86, no. 10, p. 1329–1336, doi: 10.1130/0016-7606(1975)86<1329:EMTEOT>2.0.CO;2.
- Searle, M.P., and Cox, J., 2002, Subduction zone metamorphism during formation and emplacement of the Semail ophiolite in the Oman Mountains: *Geological Magazine*, v. 129, p. 241–255.
- Sharma, M., Basu, A.R., and Nesterenko, G.V., 1992, Temporal Sr-, Nd-, and Pb-isotopic variations in the Siberian flood basalts; implications for the plume-source characteristics: *Earth and Planetary Science Letters*, v. 113, no. 3, p. 365–381, doi: 10.1016/0012-821X(92)90139-M.
- Sharp, W., 1988, Pre-Cretaceous crustal evolution of the Sierra Nevada region, California, in Ernst, W.G., ed., *Metamorphism and crustal evolution of the western United States: Rubey Volume VII*, Prentice-Hall, New Jersey, p. 824–864.
- Sharp, W.D., and Leighton, C.W., 1987, Accretion of the Foothills ophiolite, western Sierra Nevada foothills, California: *Geological Society of America Abstracts with Programs*, v. 19, no. 6, p. 450.
- Shervais, J.W., 1990, Island arc and ocean crust ophiolites; contrasts in the petrology, geochemistry and tectonic style of ophiolite assemblages in the California Coast Ranges, in Malpas, J., Moores, E., Panayiotou, A., and Xenophontos, C., eds., *Ophiolites Oceanic Crustal Analogues: Proceedings of the Symposium "Troodos 1987"*: Nicosia, Cyprus, Geological Survey Department, Ministry of Agriculture and Natural Resources, p. 507–520.
- Shervais, J.W., 2001, Birth, death, and resurrection: The life cycle of suprasubduction zone ophiolites: *Geochemistry, Geophysics, Geosystems*, v. 2, p. 2001, doi: 10.1029/2000GC000080.
- Shervais, J.W., and Kimbrough, D.L., 1985, Geochemical evidence for the tectonic setting of the Coast Range ophiolite: A composite island arc-oceanic crust terrane in western California: *Geology*, v. 13, p. 35–38, doi: 10.1130/0091-7613(1985)13<35:GEFTTS>2.0.CO;2.
- Shervais, J.W., and Kimbrough, D.L., 1987, Alkaline and transitional subalkaline metabasalts in the Franciscan Complex mélange, California, in Morris, E.M., and Pasteris, J.D., eds., *Mantle metasomatism and alkaline magmatism*: Geological Society of America Special Paper 215, p. 101–114.
- Shervais, J.W., Murchey, B.L., Kimbrough, D.L., Renne, P.R., and Hanan, B., 2005, Radioisotopic and biostratigraphic age relations in the Coast Range ophiolite, northern California: Implications for the tectonic evolution of the western Cordillera: *Geological Society of America Bulletin*, v. 117, p. 633–653.
- Sisson, V.B., and Pavlis, T.L., 1993, Geologic consequences of plate reorganization: An example from the Eocene Southern Alaska forearc: *Geology*, v. 21, no. 10, p. 913–916, doi: 10.1130/0091-7613(1993)021<0913:GCOPRA>2.3.CO;2.
- Sliter, R.V., 1984, Foraminifers from Cretaceous limestone of the Franciscan Complex, northern California, in Blake, M.C., Jr., ed., *Franciscan Geology of Northern California: Pacific Section, Society of Economic Paleontologists and Mineralogists*, v. 43, p. 149–162.
- Sliter, R.V., and McGann, M.L., 1992, Age and Correlation of the Calera Limestone in the Permanente Terrane of Northern California: *U.S. Geological Survey Open File Report OF 92-0306*, 27 p.
- Snow, C.A., Wakabayashi, J., Ernst, W.G., and Wooden, J.L., 2010, SHRIMP-based depositional ages of Franciscan metagraywackes, west-central California: *Geological Society of America Bulletin* (in press).
- Sorensen, S.S., Grossman, J.N., and Perfit, M.R., 1997, Phengite-hosted LILE enrichment in eclogite and related rocks; implications for fluid-mediated mass transfer in subduction zones and arc magma genesis: *Journal of Petrology*, v. 38, no. 1, p. 3–34, doi: 10.1093/petrology/38.1.3.
- Spray, J.G., 1984, Possible causes and consequences of upper mantle decoupling and ophiolite displacement, in Gass, I.G., Lippard, S.J., and Shelton, A.W., eds., *Ophiolites and oceanic lithosphere*, Geological Society of London Special Publication 13, p. 255–268.
- Stern, R.J., 1981, A common mantle source for western Pacific island and "hot-spot" magmas for layering in the upper mantle: *Carnegie Institute of Washington Yearbook*, v. 81, p. 455–462.
- Stern, R.J., 2004, Subduction initiation: Spontaneous and induced: *Earth and Planetary Science Letters*, v. 226, p. 275–292.
- Stern, R.J., and Bloomer, S.H., 1992, Subduction zone infancy: Examples from the Eocene Izu-Bonin-Mariana and Jurassic California arcs: *Geological Society of America Bulletin*, v. 104, p. 1621–1636, doi: 10.1130/0016-7606(1992)104<1621:SZIEFT>2.3.CO;2.
- Sun, S.S., and McDonough, W.F., 1989, Chemical and isotopic systematics of oceanic basalts: Implications for mantle composition and processes, in Saunders, A.D., and Norry, M.J., eds., *Magmatism in the ocean basins*, London: Geological Society of London Special Publication 42, p. 313–345.
- Suppe, J., and Foland, K. A., 1978, The Goat Mountain Schists and Pacific Ridge Complex: A redefined, but still intact, late Mesozoic schuppen complex, in Howell, D.G., and McDougall, K.A., eds., *Mesozoic paleogeography of the western United States, Pacific Section: Society of Economic Paleontologists and Mineralogists, Pacific Coast Paleogeography Symposium 2*, p. 431–451.
- Surpless, K.D., Graham, S.A., Covault, J.A., and Wooden, J.L., 2006, Does the Great Valley Group contain Jurassic strata? Reevaluation of the age and early evolution of a classic forearc basin: *Geology*, v. 34, p. 21–24.
- Swanson, N., Erickson, R.C., and Plummer, E., 2004, Trace element geochemistry of the Ward Creek metamorphic sequence and Big Oat Creek Metabasalt, Cazadero, CA: *Geological Society of America Abstracts with Programs*, v. 36, no. 4, p. 39.
- Tatsumi, Y., and Eggins, S., 1995, *Subduction Zone Magmatism*: Oxford, Blackwell Sciences, 211 p.
- Tatsumoto, M., 1978, Isotopic composition of lead in oceanic basalts and its implications to mantle evolution: *Earth and Planetary Science Letters*, v. 38, p. 63–87, doi: 10.1016/0012-821X(78)90126-7.
- Taylor, R.N., and Nesbitt, R.W., 1998, Isotopic characteristics of subduction fluids in an intra-oceanic setting, Izu-Bonin arc, Japan: *Earth and Planetary Science Letters*, v. 164, p. 79–98.
- Tsujimori, T., Matsumoto, K., Wakabayashi, J., and Liou, J.G., 2006, Franciscan eclogite revisited: Reevaluation of *P-T* evolution of tectonic blocks from Tiburon Peninsula, California, USA: *Mineralogy and Petrology*, v. 88, p. 243–267, doi: 10.1007/s00710-006-0157-1.
- Tsujimori, T., Liou, J.G., and Coleman, R.G., 2007, Finding of high-grade tectonic blocks from the New Idria serpentinite body, Diablo Range, California: Petrologic constraints on the tectonic evolution of an active serpentinite diapir, in Cloos, M., Carlson, W.D., Gilbert, M.C., Liou, J.G., and Sorensen, S.S., eds., *Convergent Margin Terranes and Associated Regions*: Geological Society of America Special Paper 419, p. 67–80, doi: 10.1130/3307.2419(03).
- Uehara, S., and Aoya, M., 2005, Thermal model for approach of a spreading ridge to subduction zones and its implications for high-*P*/high-*T* metamorphism: Importance of subduction versus ridge approach ratio: *Tectonics*, v. 24, doi: 10.1029/2004TC001715.
- Wakabayashi, J., 1990, Counterclockwise *P-T-t* paths from amphibolites, Franciscan Complex, California: Relics from the early stages of subduction zone metamorphism: *The Journal of Geology*, v. 98, p. 657–680, doi: 10.1086/629432.
- Wakabayashi, J., 1992, Nappes, tectonics of oblique plate convergence, and metamorphic evolution related to

- 140 million years of continuous subduction, Franciscan Complex, California: *The Journal of Geology*, v. 100, p. 19–40, doi: 10.1086/629569.
- Wakabayashi, J., 1999, Subduction and the rock record: Concepts developed in the Franciscan Complex, California, *in* Sloan, D., Moores, E.M., and Stout, D., eds., *Classic Cordilleran Concepts: A View from California*: Geological Society of America Special Paper 338, p. 123–133.
- Wakabayashi, J., and Deino, A., 1989, Laser-probe $^{40}\text{Ar}/^{39}\text{Ar}$ ages from high-grade blocks and coherent blueschists, Franciscan Complex, California: Preliminary results and implications for Franciscan tectonics: *Geological Society of America Abstracts with Programs*, v. 21, no. 6, p. A267.
- Wakabayashi, J., and Dilek, Y., 1987, An alpine-style collision in the northern Sierra Nevada, California: Structural and metamorphic evidence: *EOS Transactions of the American Geophysical Union Fall Meeting Supplement*, v. 68, no. 44, p. 1474.
- Wakabayashi, J., and Dilek, Y., 2000, Spatial and temporal relations between ophiolites and their subophiolitic soles: A test of models of forearc ophiolite genesis, *in* Dilek, Y., Moores, E.M., Elthon, D., and Nicolas, A., eds., *Ophiolites and Oceanic Crust: New Insights from Field Studies and Ocean Drilling*: Geological Society of America Special Paper 349, p. 53–64.
- Wakabayashi, J., and Dilek, Y., 2003, What constitutes “emplacement” of an ophiolite?: Mechanisms and relationship to subduction initiation and formation of metamorphic soles, *in* Dilek, Y., and Robinson, P.T., eds., *Ophiolites in Earth History*: Geological Society of London Special Publication 218, p. 427–447.
- Wakabayashi, J., and Dumitru, T.A., 2007, $^{40}\text{Ar}/^{39}\text{Ar}$ ages from coherent high-pressure metamorphic rocks of the Franciscan Complex, California: Revisiting the timing of metamorphism of the world’s type subduction complex: *International Geology Review*, v. 49, p. 873–906, doi: 10.2747/0020-6814.49.10.873.
- White, W.M., Hofmann, A.W., and Puchelt, H., 1987, Isotope geochemistry of Pacific mid-ocean ridge basalt: *Journal of Geophysical Research*, v. 92, no. B6, p. 4881–4893, doi: 10.1029/JB092iB06p04881.
- Williams, H., and Smyth, W.R., 1973, Metamorphic aureoles beneath ophiolite suites and alpine peridotites: Tectonic implications with west Newfoundland example: *American Journal of Science*, v. 273, p. 594–621.
- Zagorevski, A., Rogers, N., van Staal, C.R., McNicoll, V., Lissenberg, C.J., and Valverde-Vaquero, P., 2006, Lower to Middle Ordovician evolution of peri-Laurentian arc and backarc complexes in the Iapetus: Constraints from the Annieopsquotch accretionary tract, central Newfoundland: *Geological Society of America Bulletin*, v. 118, p. 324–342, doi: 10.1130/B25775.1.

MANUSCRIPT RECEIVED 28 JANUARY 2009

REVISED MANUSCRIPT RECEIVED 10 JULY 2009

MANUSCRIPT ACCEPTED 15 JULY 2009

Printed in the USA